



Pharmacological induction of Heat Shock Protein 70 by celastrol protects motoneurons from excitotoxicity in rat spinal cord in vitro

Antonela Petrović^{1,2} | Jaspreet Kaur² | Ivana Tomljanović¹ | Andrea Nistri²  |
Miranda Mladinic¹ 

¹Department of Biotechnology, University of Rijeka, Rijeka, Croatia

²Neuroscience Department, International School for Advanced Studies (SISSA), Trieste, Italy

Correspondence

Miranda Mladinic, Department of Biotechnology, University of Rijeka, Rijeka, Croatia.

Email: mirandamp@uniri.hr

Present address

Jaspreet Kaur, Institute of Neurosciences of Timone - CERIMED, UMR 7289, Aix-Marseille University, Marseille, France.

Funding information

Hrvatska Zaklada za Znanost, Grant/Award Number: IP-2016-06-7060; International Centre for Genetic Engineering and Biotechnology, Grant/Award Number: CRP/CRO14-03; European Regional Development Fund

Abstract

The secondary phase of spinal cord injury arising after the primary lesion largely extends the damage severity with delayed negative consequences for sensory-motor pathways. It is, therefore, important to find out if enhancing intrinsic mechanisms of neuroprotection can spare motoneurons that are very vulnerable cells. This issue was investigated with an in vitro model of rat spinal cord excitotoxicity monitored for up to 24 hr after the primary injury evoked by kainate. This study sought to pharmacologically boost the expression of heat shock proteins (HSP) to protect spinal motoneurons using celastrol to investigate if the rat spinal cord can upregulate HSP as neuroprotective mechanism. Despite its narrow range of drug safety in vitro, celastrol was not toxic to the rat spinal cord at 0.75 μ M concentration and enhanced the expression of HSP70 by motoneurons. When celastrol was applied either before or after kainate, the number of dead motoneurons was significantly decreased and the nuclear localization of the cell death biomarker AIF strongly inhibited. Nevertheless, electrophysiological recording showed that protection of lumbar motor networks by celastrol was rather limited as reflex activity was impaired and fictive locomotion largely depressed, suggesting that functional deficit persisted, though the networks could express slow rhythmic oscillations. While our data do not exclude further recovery at later times beyond the experimental observations, the present results indicate that the upregulated expression of HSP in the aftermath of acute injury may be an interesting avenue for early protection of spinal motoneurons.

KEYWORDS

heat shock proteins, neonatal rat spinal cord preparation in vitro, nuclear apoptosis-inducing factor, spinal cord injury, spinal motoneurons

Abbreviations: 5-HT, *N*-methyl-D-aspartate; AIF, apoptosis-inducing factor; DAPI, 4',6-diamidino-2-phenylindole; DTT, dithiothreitol; EDTA, ethylenediaminetetraacetic acid; FL, fictive locomotion; HSFs, heat shock transcription factors; HSP, heat shock protein; HSR, heat shock response; nAIF, nuclear apoptosis-inducing factor; NEAA, nonessential amino acids; NMDA, *N*-methyl-D-aspartate; PBS, phosphate buffered saline; PFA, paraformaldehyde; *p*, probability; ROI, region of interest; RT, room temperature; SCI, spinal cord injury; SDS-PAGE, sodium dodecyl sulfate – polyacrylamide gel electrophoresis; SDS, sodium dodecyl sulfate; VRs, ventral roots.

Edited by Ying-Shing Chan. Reviewed by Melissa Andrews and Melissa Andrews.

All peer review communications can be found with the online version of the article.

1 | INTRODUCTION

In vivo and in vitro studies have shown that, following spinal cord injury (SCI), a substantial number of spinal neurons survive despite severe symptoms of motor and sensory deficit arising from the secondary lesion process that extends, within the first 24 hr, the pathological degeneration to initially spared spinal areas (Ahuja et al., 2017; Dell'Anno & Strittmatter, 2017; Filous & Schwab, 2018; Kuzhandaivel, Nistri, Mazzone, & Mladinic, 2011; Quraishe, Forbes, & Andrews, 2018). This observation is corroborated by clinical studies (Hoh, Mercier, Hussey, & Lane, 2013; Kaelan, Jacobsen, & Kakulas, 1988; Squair, West, & Krassioukov, 2015). The question then arises about the nature of the intrinsic protective mechanisms that can avoid a more extensive neuronal damage.

The heat shock response (HSR), which occurs when cells are exposed to stress or injury, is a major defense mechanism evolutionary conserved among species. HSR starts with translocation of stress-induced heat shock transcription factors (HSFs) to the nucleus to bind heat shock promoter elements, and to induce the expression of the chaperone heat shock proteins (HSP) to prevent neurodegeneration by inhibiting the formation of aberrant proteins (Batulan et al., 2003; Muchowski & Wacker, 2005). HSP70 is one of these chaperones and plays an important role in general neuroprotection (Muchowski, 2002). HSP70 has the anti-apoptotic ability to inhibit both Apaf-1-mediated caspase-dependent and the apoptosis-inducing factor (AIF)-mediated caspase-independent programmed cell death by binding to and neutralizing these two pro-apoptotic proteins (Ravagnan et al., 2001; Turturici, Sconzo, & Geraci, 2011).

Thus, HSP70 has been proposed to play a role in the spinal cord lesion pathophysiology although evidence remains circumstantial (Reddy, La Marca, & Park, 2008). Thus, higher levels of HSPs have been detected in the cerebrospinal liquid of dogs with spinal cord injury (Awad et al., 2008). In our former report (Shabbir et al., 2015) using an in vitro spinal cord model simulating the excitotoxic damage developing as an early consequence of spinal injury, we observed that motoneurons able to survive this insult usually expressed high levels of HSP70. Furthermore, pharmacological inhibition of HSP70 intensified neuronal losses, especially motoneuronal death (Shabbir et al., 2015). Motoneurons have an unusually high threshold for the stress-induced activation of the heat shock response. This ineffectiveness of motoneurons to trigger the HSR may result in an increased aberrant protein folding and higher sensitivity to stress (Batulan et al., 2003; Kalmar & Greensmith, 2009). To overcome this drawback, extracellular HSP70 may be necessary to assist cell survival (Fleshner & Johnson, 2005; Robinson, 2005; Tytell, 2005).

Celastrol is a chemical compound isolated from the root extracts of *Tripterygium wilfordii*, known also as Thunder of God vine, belonging to the Celastraceae family. Its chemical structure is a pentacyclic triterpenoid. Extracts of *T. wilfordii* have been used as traditional herbal medicine to treat many conditions, including fever, chills, edema, and joint pain. The plant is autochthonous in Southern China (Allison, Cacabelos, Lombardi, Alvarez, & Vigo, 2001).

While celastrol is known for its anti-inflammatory and anti-tumor properties (Zhang et al., 2008), its mode of action and cellular targets are incompletely understood. Celastrol leads to induction of HSP, which play an important role in prevention of unwanted protein aggregation within cells (Salminen, Lehtonen, Paimela, & Kaarniranta, 2010). In particular, HSP70 induction is reported to ameliorate pathological changes of neurodegenerative diseases and inflammation (Ran et al., 2004).

Celastrol has been tested as a neuroprotectant in various models of neurodegeneration with a beneficial outcome (Deane & Brown, 2018; Faust et al., 2009; Gu et al., 2018; Jantas et al., 2013; Kyung et al., 2015; Sun et al., 2010; Xu et al., 2017; Zhang et al., 2017) by inducing rapid HSP70 expression (Allison et al., 2001; Cascão, Fonseca, & Moita, 2017; Chow & Brown, 2007; DeMeester, Buchman, & Cobb, 2001; Kannaiyan, Shanmugam, & Sethi, 2011; Salminen et al., 2010; Traynor et al., 2006; Trott et al., 2008; Welsh, Moyer, & Harris, 1992; Westerheide et al., 2004). Its action on spinal excitotoxicity remains, however, to be studied. Celastrol hyperphosphorylates HSF1, thereby increasing the HSF1 DNA-binding affinity and inducing the transcription of HSP-genes. The kinetics of HSF1 are similar for both stress and celastrol-induced activation (Trott et al., 2008; Turturici et al., 2011). Activated HSF1 in trimeric form undergoes nuclear localization and transactivates gene expression, leading to the expression of the inducible form of HSP70 protein (HSP72; Boridy, Le, Petrecca, & Maysinger, 2014).

In this study, the ability of celastrol to upregulate HSP70 expression and protect motoneurons from kainate-evoked excitotoxicity was explored by using the validated model of neonatal rat SCI in vitro (Bianchetti, Mladinic, & Nistri, 2013; Kuzhandaivel, Margaryan, Nistri, & Mladinic, 2010; Kuzhandaivel, Nistri, & Mladinic, 2010; Margaryan, Mattioli, Mladinic, & Nistri, 2010; Margaryan, Mladinic, Mattioli, & Nistri, 2009; Mladinic, Bianchetti, Dekanic, Mazzone, & Nistri, 2014; Nasrabad, Kuzhandaivel, Mladinic, & Nistri, 2011; Shabbir et al., 2015; Taccola, Margaryan, Mladinic, & Nistri, 2008; Taccola, Mladinic, & Nistri, 2010). This preparation is advantageous because it allows recording the output of the locomotor networks expressed as fictive locomotion for up to 24 hr (Margaryan et al., 2009, 2010; Nasrabad et al., 2011; Shabbir et al., 2015; Taccola et al., 2008, 2010). Our model consists of transient (1 hr) application of kainate followed by extensive washout (6–24 hr) to enable monitoring

structural and functional consequences to motor networks during the critical secondary phase of SCI. The experimental protocol is designed to resemble the primary lesion (during which excitotoxicity develops) and the subsequent delivery of intensive care and life support later given in clinical settings (Mehta, Prabhakar, Kumar, Deshmukh, & Sharma, 2013; Park, Velumian, & Fehlings, 2004). Two distinct experimental strategies were used, namely administration of celastrol either before or after the excitotoxic stimulus. Preapplication of celastrol would, of course, not mimic any clinical setting, yet it might cast light on the question whether amplifying the HSP70 expression may confer additional resistance to damage. On the other hand, delayed application would clarify if neuronal death that occurs over the next few hours after kainate application can be slowed down and/or dampened by larger expression of HSP70 or its time-mismatch would cause lesion progression.

2 | MATERIALS AND METHODS

2.1 | Neonatal rat spinal cord preparation

All dissections were performed at the International School for Advanced Studies (SISSA), in accordance with the National Institutes of Health guidelines for the care and use

of laboratory animals (NIH Publications No. 80-23, revised 1996) and the Italian act D. Lgs. 27/1/92 no. 116 (implementing the European Community directives no. 86/609 and 2010/63/EU). The ethics committee of SISSA approved all experimental protocols. All efforts were directed to reduce the number of animals used and minimize their suffering.

Neonatal 0–2-day old Wistar rats (Harlan Laboratories, S. Pietro al Natissone, Udine), of randomly distributed gender, were sacrificed by decapitation under terminal urethane anesthesia (0.2 ml i.p. of a 10% w/v solution). Spinal cords were dissected out in oxygenated Krebs solution: 113 mM NaCl, 4.5 mM KCl, 1 mM MgCl₂·6H₂O, 2 mM CaCl₂, 1 mM NaH₂PO₄, 25 mM NaHCO₃, 11 mM glucose, continuously gassed with 95% O₂, 5% CO₂; pH 7.4 at room temperature (RT) and placed in experimental chambers for various lengths of time as indicated later. All drugs were administered by tissue superfusion. Full details of the experimental procedures have been previously published (Taccola et al., 2008, 2010).

2.2 | Neuroblastoma cells

SH-SY5Y (ATCC) were cultured in 1:1 mixture of Eagle's Minimum Essential Medium and F12 Medium, 1% Nonessential Amino Acids (NEAA), 1% penicillin/streptomycin with a fetal bovine serum to a final concentration of

TABLE 1 Antibodies used in immunohistochemistry and western blotting

Name	Immunogen	ManufacturerCatalog #Lot #RRID #	Species and type	Dilution
Anti-neuronal Nuclei, clone EPR12763 (NeuN)	Synthetic peptide within Human NeuN aa 1-100 (Cysteine residue). Protein A purified.	Abcam ab177487 GR249899-46 AB_2532109	Rabbit monoclonal	IHC 1:500
Anti-apoptosis-Inducing Factor (AIF)	KLH-conjugated synthetic peptide corresponding to the C-terminal region of human AIF	Millipore 04-430 2435042 AB_673048	Rabbit monoclonal	IHC 1:100
Anti-neurofilament H Nonphosphorylated (SMI-32)	Homogenized hypothalami from Fischer 344 rat brain	Millipore NE1023 D00168792 AB_2043449	Mouse monoclonal	IHC 1:500
Anti-choline Acetyltransferase (ChAT)	Human placental enzyme. Affinity purified	Millipore AB144P 2620146 AB_2079751	Goat polyclonal	IHC 1:100
Anti-heat shock Protein 70, clone BRM-22 (HSP70)	Purified full length native HSP 70/HSC 70 of bovine origin	Abcam ab6535 656321 AB_305549	Mouse monoclonal	IHC 1:400
Anti-cytosolic stress-induced Heat Shock Protein 70, clone C92F3A-5 (HSP72)	Native human HSP70 protein. Protein G affinity purified	Enzo Life Sciences ADI-SPA 810 09021453 AB_2039263	Mouse monoclonal	WB 1:1000

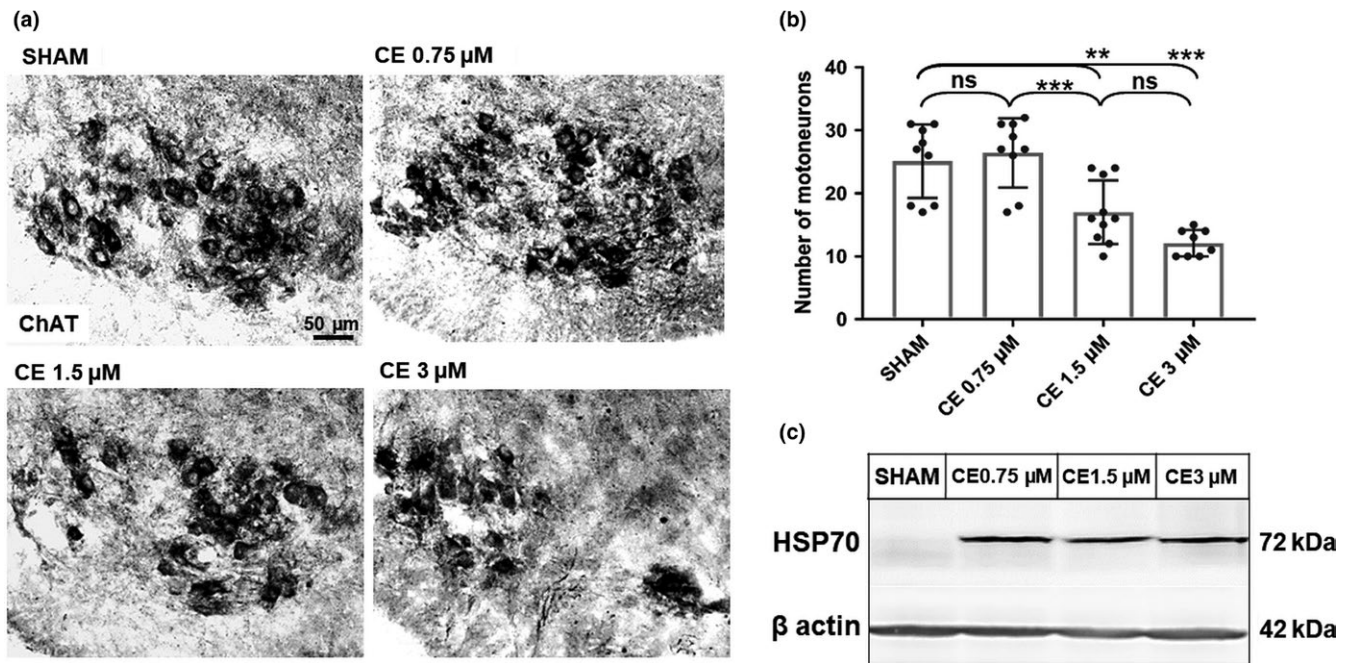


FIGURE 1 Motoneuronal numbers and HSP70 expression after 6 hr application of celastrol at 37°C. (a) Spinal cord sections (16 µm) were immuno-stained for ChAT to visualize motoneurons in untreated sham preparations or in preparations treated with different celastrol (CE) concentrations. Motoneuronal deterioration and death (white empty zones) are visible in preparations treated with 1.5 or 3 µM celastrol. (b) Bar graph shows the average number of motoneurons counted in the ventral horn ROI. Datapoints show value scattering in each histological section. Number of motoneurons is significantly lower following celastrol concentrations higher than 0.75 µM, when compared to sham preparations. One-way ANOVA followed by Holm–Sidak multiple comparisons test. $F_{3,32} = 16.42$, $p < 0.001^{***}$. SHAM vs CE 1.5 µM $p = 0.003^{**}$; SHAM vs CE 3 µM $p < 0.001^{***}$; CE 0.75 µM vs CE 1.5 µM $p < 0.001^{***}$; averaged data from three sections for each spinal cord in each experimental group comprising three spinal cords. Data are mean \pm SD. Scale bar = 50 µm. (c) Western analysis of inducible HSP70 levels in the rat spinal cord. Note that under sham conditions spinal cord expresses no inducible HSP70 in contrast to elevated levels after application of celastrol (0.75, 1.5 and 3 µM)

10% (Deng, Shi, Liu, & Qu, 2013). Twenty-four hours after seeding, cells were treated with 0.75 µM celastrol at different time points (2–24 hr) to test the celastrol ability to increase HSP70 levels (at 37°C). After celastrol treatment, cells were harvested with Laemmli sample buffer (1% bromophenol blue, 1 M DTT, 10% SDS and 1 M Tris-Cl pH 6.8, supplemented with protease inhibitor cocktail) and processed for western blotting as described in the methods below. Figure S1 shows the time-dependent expression of inducible HSP. Based on these data demonstrating already robust expression (approximately three times more than in untreated cells) of inducible HSP70 at 6 hr, we applied celastrol for this length of time to the spinal cord in vitro.

2.3 | Spinal cord drug protocols

First, we looked for potential toxicity of celastrol (Tocris Bioscience, Bristol, UK; Cat. No. 3203); thus, control spinal cords were exposed to three celastrol concentrations (0.75, 1.5 and 3 µM) for 6 hr at 37°C and subsequently examined for motoneuron survival (see Figure 1a,b). To mimic the excitotoxic component of SCI, the glutamate analogue kainate (Tocris Bioscience; Cat No. 0222) was applied to in vitro

spinal cord preparations at 50 µM concentration for 1 hr at 37°C or room temperature (RT; 22–23°C) and washed out with Krebs solution (Mazzone et al., 2010). Lastly, to investigate the potential neuroprotective effects of celastrol, rat spinal cord in vitro preparations were treated with 0.75 µM celastrol either 6 hr before (and washout prior to kainate) or for 6 hr after kainate-induced injury at the temperature indicated in the Results section.

Control spinal cords were either used immediately after dissection for immunohistochemistry (freshly fixed tissue) or kept in oxygenated Krebs solution (sham preparations) at the temperature indicated in the Results sections. These sham preparations were always processed in parallel with experimentally treated spinal cords.

2.4 | Immunohistochemistry

Full details of this procedure have been previously published (Bianchetti et al., 2013; Taccola et al., 2008, 2010). In brief, spinal cords were fixed in 4% PFA dissolved in phosphate-buffered saline (PBS) for 12–24 hr at 4°C, followed by 24 hr immersion in 30% sucrose for cryoprotection. Lumbar spinal cord segments from T13–L3 were cut into 16 µm

thin sections, using the sliding cryostat Bright OTF5000 (BioOptica, Milan, Italy) and mounted on Superfrost Plus glasses (Menzer-Glaser, Braunschweig, Germany).

For immunostaining, the tissue sections were first treated with blocking solution containing 3% fetal bovine serum (Gibco, Thermo Fisher Scientific, Waltham, MA, USA), 3% bovine serum albumin and 0.3% Triton X-100 (Sigma-Aldrich, St. Louis, MO, USA) in PBS for 1 hr at room temperature. After blocking, sections were incubated with primary antibodies (Table 1) in a solution containing 1% fetal bovine serum, 1% bovine serum albumin, 0.1% Triton (overnight at 4°C). Primary antibodies used were targeting AIF (Millipore, 04-430, 1:100), HSP70 (Abcam, ab6535, 1:400), NeuN (Abcam, ab177487, 1:500), SMI32 (Millipore, NE1023, 1:500) and ChAT (Millipore, AB144P, 1:100). These primary antibodies were previously tested and validated on neonatal rat spinal cord tissue in our laboratory (Deumens, Mazzone, & Taccola, 2013; Mladinic, Nistri, & Taccola, 2013) as shown in previous studies with AIF (Shabbir et al., 2015), NeuN and SMI32 (Bianchetti et al., 2013; Kuzhandaivel, Margaryan et al., 2010; Kuzhandaivel, Nistri et al., 2010; Taccola et al., 2008, 2010). The secondary antibodies were Alexa Fluor Plus 488, 555 or 594 (1:500 dilution; Invitrogen, Milan, Italy). After the secondary antibody incubation (2 hr at RT), spinal cord sections were incubated in 1 µg/ml solution of 4,6-diamidino-2-phenylindole (DAPI) for 20 min to visualize cell nuclei and mounted on glass slides with DAKO mounting medium (Carpinteria, CA, USA).

Sections from T12 to L3 segments were chosen for analysis because this spinal cord region contains the locomotor central pattern generator (Kiehn, 2006). Lumbar motoneurons were analyzed in the region of interest (ROI; 250 × 250 µm) of the ventral horn using the procedure for their identification and counting validated previously (Cifra, Mazzone, Nani, Nistri, & Mladinic, 2012). A similar size of ROI was used for counting neurons in the central and dorsal regions. Three experimental sets each comprising seven spinal cords in different conditions (freshly frozen, FF; SHAM; 50 µM kainate, KA50; 6 hr application of celastrol, CE 6 hr; 24 hr application of celastrol, CE 24 hr; preapplication of celastrol (6 hr) followed by kainate (1 hr), CE 6 hr + KA50; application of kainate (1 hr) followed by 6–24 hr application of celastrol, KA50 + CE 6–24 hr) were employed. Three to five sections per spinal cord were analyzed for each experimental group. Immunofluorescent staining was analyzed with Olympus IX83 microscope and CellSense software (Olympus, Tokyo, Japan) using the 20× UPLFLN (AN 0, 5) and 40× OUPFLN (AN 1, 30) objectives. All experimental groups were processed in parallel and immunohistochemistry procedures were done simultaneously. Imaging was performed using identical parameters for each channel (40× magnification, exposure time: HSP70 100 ms; NeuN 50 ms; DAPI 35 ms,

0.5 µm step size). The HSP70 intensity was measured over the whole area of single motoneurons and averaged for each group. Furthermore, CellSense line scan tool was used for analysis of HSP70 cellular distribution in six representative motoneurons from cells in which HSP70 intensity had previously been measured over the whole cell area. The average value of each channel was finally shown as a line plot.

2.5 | Western blot

As previously reported (Bianchetti et al., 2013; Kuzhandaivel, Nistri et al., 2010), the whole spinal cord tissue (three spinal cords for each group in three experiments) was lysed with CHAPS Lysis buffer (0.5% CHAPS, 50 mM Tris pH 7.5, 1 mM EDTA, 150 mM NaCl, 10% glycerol + protease inhibitor, 1:50; Roche, Basel, Switzerland) and incubated for 5 min on ice. Tissue lysates were sonicated 3 × 10 min and centrifuged for 1 min at 1,000 g at RT. Precipitation was performed with acetone (ice-cold acetone was added to one volume of protein sample and mixture was vortexed and incubated at –20°C overnight). After centrifugation at 1000 g for 15 min at 4°C, the supernatant was discarded, and the pellet was air-dried. The protein pellets were then resuspended in 25 µl of Laemmli sample buffer (1% Bromophenol blue, 1 M DTT, 10% SDS and 1 M Tris-Cl pH 6.8), vortexed and put in the thermo shaker for one hr at 37°C. 1-D SDS-PAGE electrophoresis was performed with 4% stacking gel and 10% resolving gel (Mini-Protean Tetra Cell; Bio-Rad, CA, USA). Before loading, the samples were heated at 95°C for 5 min. Fifty micrograms of proteins were loaded on the gel and transferred to nitrocellulose membrane. For detection, Ponceau S stain was used. After blocking in 4% nonfat milk, membranes were probed with primary antibodies raised against inducible form of HSP70 (ADI-SPA-810; Enzo Life Sciences, New York, USA) overnight at 4°C (Table 1). After washing in Tris-buffered saline (TBS) with Tween 20, membranes were incubated with secondary antibody one hr at RT. The signal was visualized with Western Lightening Chemiluminescence Reagent Plus Kit (Perkin Elmer, MA, USA) and the densitometric analysis was performed by Quantity One software (Bio-Rad, CA, USA). To normalize the HSP70 signal, membrane was incubated for 20 min with HRP-conjugated β-actin (A3854 1:10,000, Sigma-Aldrich).

2.6 | Electrophysiological analysis

Recordings were obtained at room temperature from pairs of lumbar L2 and L5 ventral roots (VRs) which express the activity of flexor and extensor motor pools to hind limbs, respectively (Taccola & Nistri, 2006; Taccola et al., 2008). Low threshold VR reflexes were evoked by square pulses (0.1 ms) to a single dorsal root by straddling threshold and detecting the smallest response in ipsilateral (and ipsi-segmental) VRs: this method is

suitable to induce monosynaptic reflexes as long as the stimulus intensity is <1.5 threshold (Kaur, Rauti, & Nistri, 2018; Ostroumov, Grandolfo, & Nistri, 2007). This approach is consistent with *in vivo* recording from motoneurons together with recording of incoming primary afferent signals whereby increments of stimulus intensity above threshold, yet below 1.5 times elicit monosynaptic excitatory potentials (Krnjević, Lamour, MacDonald, & Nistri, 1979). Furthermore, the monosynaptic origin was assumed on the basis of the shortest latency and relatively constant amplitude after low frequency stimulation (Fulton & Walton, 1986). Polysynaptic reflexes were elicited by $3\times$ threshold intensity (Kaur et al., 2018). Threshold values for ventral root responses were systematically analyzed prior, during and at the end of each recording session. All responses were analyzed by averaging the amplitude (measured from baseline to peak) and area (measured as area under a 20 s long response) of 3–5 events (Taccola et al., 2008). To induce cumulative depolarization with superimposed alternating oscillations typical of electrically evoked fictive locomotion (Marchetti, Beato, & Nistri, 2001), 30 pulses (2 Hz, same stimulus intensity as above) were applied to a single dorsal root. Chemically induced fictive locomotion was induced by bath-applied *N*-methyl-D-aspartate (NMDA) (3–6 μM) and 5-hydroxytryptamine (5-HT) (10 μM) (Cazalets, Sqalli-Houssaini, & Clarac, 1992). Standard definitions of fictive locomotion (alternating rhythmic discharges among flexor and extensor motor pools) and oscillations (rapid deflections from the baseline at regular periodicity) were provided by Cazalets et al. (1992), Marchetti et al. (2001) and Kaur et al. (2018). Signals were acquired and processed with PCLAMP software 9.2 (Molecular Devices, Sunnyvale, CA, USA). Amplitude and periodicity of fictive locomotor rhythms were measured as reported earlier (Taccola et al., 2008).

2.7 | Data analysis

Results are presented as scatter plot with mean \pm SD. Statistical analysis was performed using GRAPHPAD PRISM 7.04 (GraphPad Software Inc., CA, USA).

D'Agostino–Pearson normality test was used to calculate how far the values differ from the value expected with a Gaussian distribution. Brown–Forsythe test was used to test the assumption that all data are sampled from populations with the same standard deviations. One-way ANOVA was used to compare three or more data groups, based on the assumption that the populations are Gaussian and that variances are equal. Following one-way ANOVA parametric test, Holm–Šidák test was used for multiple comparisons between two data groups.

Data groups with different variances that fail a normality test were compared using the Kruskal–Wallis test. Following Kruskal–Wallis nonparametric test, Dunn's multiple comparisons test was used to compare the difference in the sum of ranks between two data groups with the expected average difference.

T test was used when comparing two normally distributed data groups. The *t* test assumption that the two samples come from populations that have identical standard deviations was tested using the *F* test.

The accepted level of significance was $p < 0.05$, $p < 0.001$ Very significant***; 0.001–0.01 Very significant**; 0.01–0.05 Significant*; ≥ 0.05 Not significant. Decimal format used to report *p* values was according to the recommended NEJM (New England Journal of Medicine) style. (https://www.graphpad.com/guides/prism/7/statistics/index.htm?stat_decimal_formatting_of_p_values.htm; https://www.graphpad.com/guides/prism/7/statistics/index.htm?extremely_significant_results.htm).

3 | RESULTS

3.1 | Effect of celastrol on motoneurons in control condition

Before testing the neuroprotective action of celastrol, we looked for any neurotoxicity of celastrol on rat spinal cord because previous studies have shown toxic effects of this drug (3 μM) on primary neuronal cultures (Chow & Brown, 2007; Kalmar & Greensmith, 2009). After applying celastrol (0.75, 1.5 and 3 μM) for 6 hr at 37°C, lumbar sections were immunostained for ChAT to visualize motoneurons identified as large ($>20 \mu\text{m}$) ventral horn cells immunopositive to ChAT or SMI32 because both markers provide similar yields (Cifra et al., 2012). The average number of motoneurons per ROI was unchanged after 0.75 μM celastrol (CE 0.75 μM) (Figure 1a,b). However, when the celastrol concentration was higher (CE 1.5 μM ; 3 μM), the number of motoneurons was significantly lower (ANOVA; *** $p \leq 0.001$; 30–50% reduction) in treated preparations when compared to sham preparations kept for 6 hr *in vitro* (Figure 1a,b). We also investigated the levels of inducible form of HSP70, using western blot analysis. Thus, in celastrol-treated preparations (CE 0.75 μM ; CE 1.5 μM ; CE 3 μM), (0.75, 1.5 and 3 μM concentrations), ostensibly higher expression of the inducible HSP70 was detected compared to sham preparations (Figure 1c). Additionally, we confirmed the ability by 0.75 μM celastrol to induce sustained production of HSP70 for 24 hr in the neuroblastoma cell line SH-SY5Y (Figure S1) and to be free of neurotoxicity even on neurons counted in ROIs of the ventral, central, and dorsal areas (Figure S2). Thus, 0.75 μM was taken as a suitable concentration of celastrol for neuroprotection analysis as toxicity appears unrelated to HSP70 expression and its origin remains to be studied (Chow & Brown, 2007; Kalmar & Greensmith, 2009).

3.2 | Celastrol contributes to survival of motoneurons

We tested the celastrol ability to induce HSP70 protein and to protect lumbar motoneurons after excitotoxic insult using the neonatal

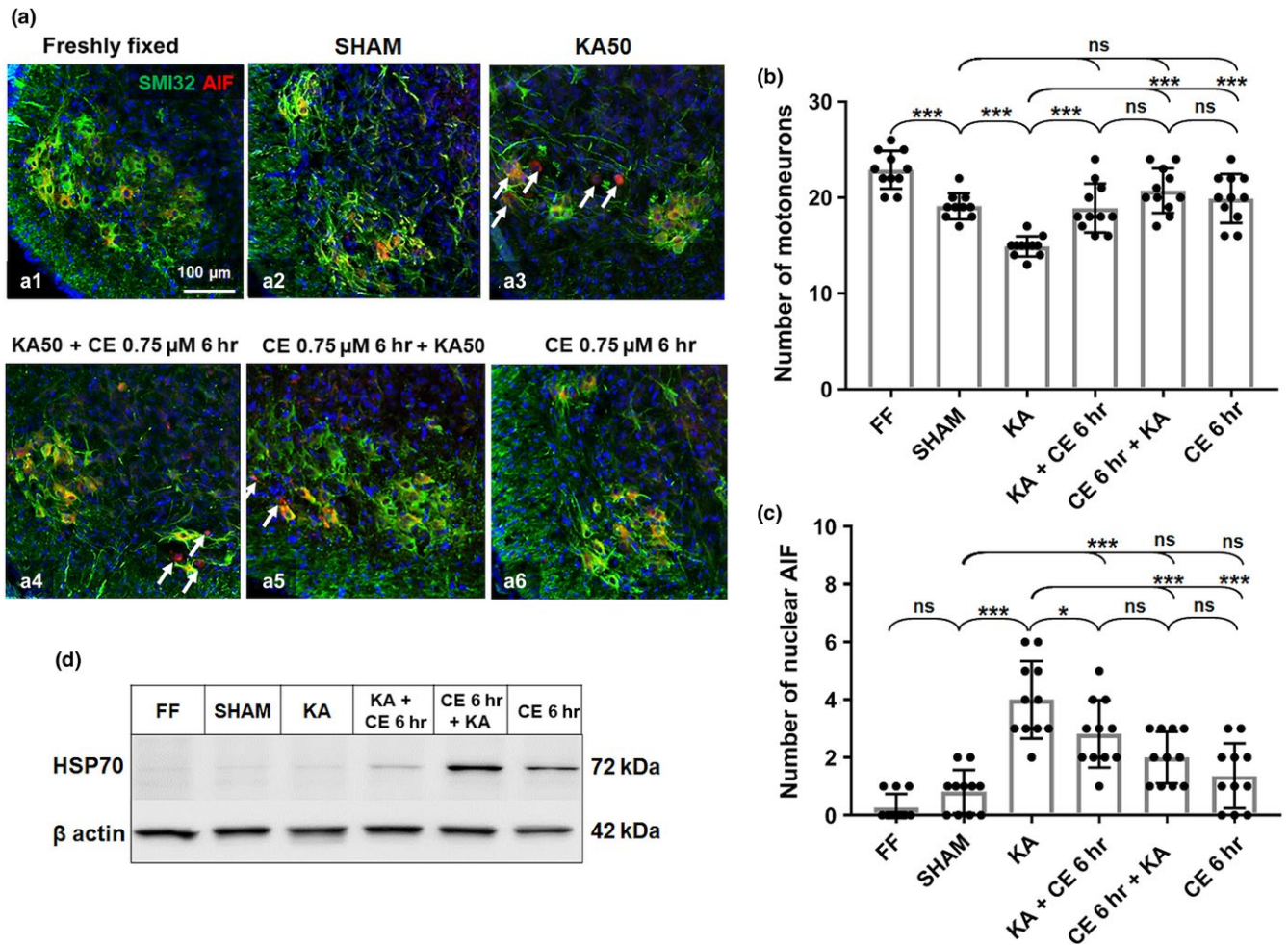


FIGURE 2 Celastrol mediated reduction in nAIF translocation in motoneurons after excitotoxic insult. (a) Examples of spinal cord sections after treatment with celastrol and/or kainate in vitro at 37°C. Motoneurons were immunostained with SMI32 (green), while nAIF immunostaining (red) was taken as an index of cell death. Cell nuclei were stained with DAPI (blue). (a) freshly fixed tissue (a1), tissue kept in sham condition (a2), or after the following protocols: treated with 50 μM kainate for 1 hr (a3), 0.75 μM celastrol (CE) for 6 hr (a4), pretreated with 0.75 μM celastrol followed by kainate application (a5) or 0.75 μM celastrol after kainate (a6). Red arrows indicate examples of nAIF (nAIF). Note fewer motoneurons with nAIF with celastrol application (a5, a6) when compared with no celastrol treatment after kainate (a3). Scale bar is 100 μm. (b) The bar graph represents the numbers of motoneurons with cytoplasmic AIF and nAIF for the experimental conditions shown in a1–a6. Note the change in motoneuronal number 6 hr after various experimental protocols at 37°C. Following the kainate-induced injury number of motoneurons decreased. Celastrol application, both before or after kainate application, preserved the number of motoneurons. One-Way ANOVA followed by Holm–Sidak multiple comparisons test. $F_{5,59} = 18.03, p < 0.001^{***}$. FF vs SHAM $p < 0.001^{***}$; SHAM vs KA $p < 0.001^{***}$; KA vs CE 6 hr $p < 0.001^{***}$; KA vs CE 6 hr + KA $p < 0.001^{***}$; KA vs KA + CE 6 hr $p < 0.001^{***}$; averaged data from three to four sections for each spinal cord in each experimental group comprising three spinal cords. Data are mean ± SD. (c) the numbers of motoneurons containing nAIF for the experimental conditions shown in a1–a6. Following kainate application, number of motoneurons containing nAIF increased. Celastrol application, either before or after kainate, decreased the number of motoneurons with nAIF translocations. One-way ANOVA followed by Holm–Sidak multiple comparisons test. $F_{5,60} = 20.49, p < 0.001^{***}$. SHAM vs KA $p < 0.001^{***}$; SHAM vs KA + CE 6 hr $p < 0.001^{***}$; KA vs CE 6 hr $p < 0.001^{***}$; KA vs CE 6 hr + KA $p < 0.001^{***}$; KA vs KA + CE 24 hr $p = 0.02^*$. Same samples as in (b). (d) Western analysis of inducible HSP70 levels in the rat spinal cord carried out 6 hr after the following protocols: freshly frozen spinal cords (FF), sham, kainate, kainate followed by celastrol, celastrol pretreatment followed by kainate, and treated with celastrol only. Note that freshly dissected spinal cords or kept in sham conditions did not express inducible HSP70, the same as kainate treated spinal cords. Spinal cords pretreated with celastrol or treated with celastrol alone expressed elevated levels of inducible HSP70. Application of celastrol after kainate led to slight elevation of inducible HSP70. Three western blots were performed for each group. Equal loading was confirmed with β-actin blotting (bottom lane)

rat spinal cord in vitro at two different temperatures, namely 37°C or room temperature. Previous experiments have shown that room temperature is necessary for prolonged recording of network

activity that rapidly declines at ≥33°C (Taccola & Nistri, 2005), while higher temperature favors the expression of HSP (Batulan et al., 2003; Muchowski & Wacker, 2005).

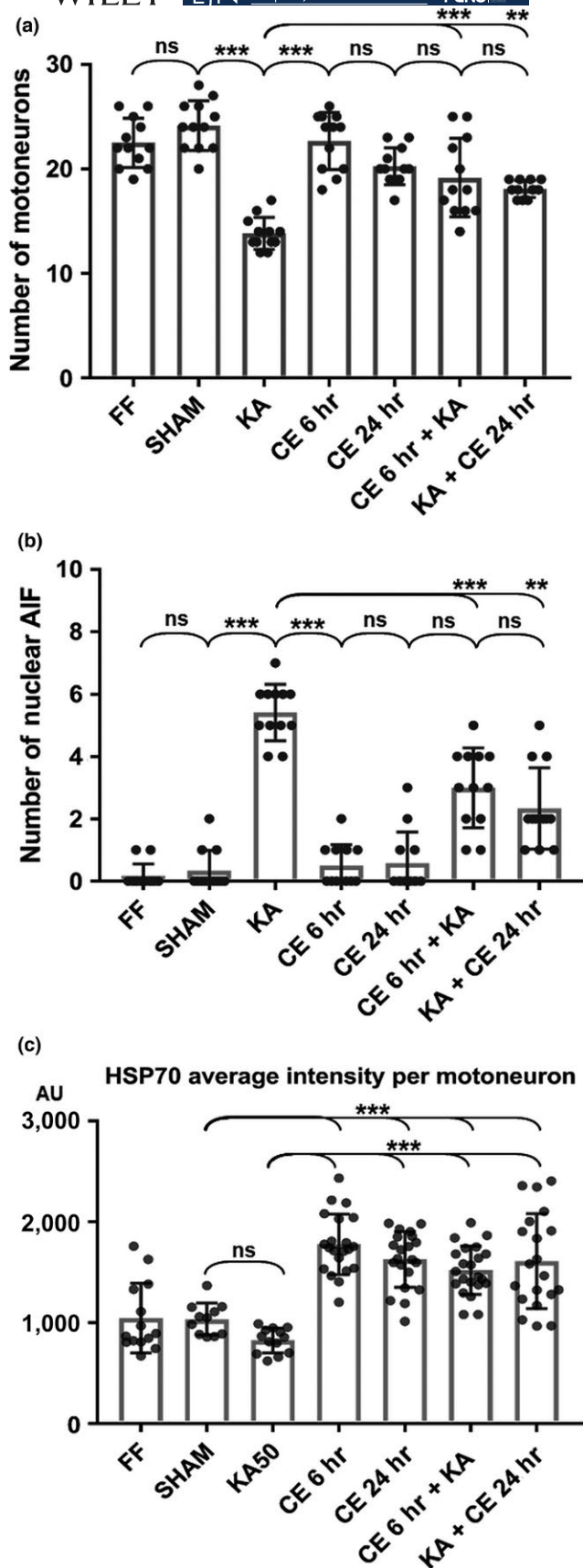


FIGURE 3 Effect of celastrol on excitotoxicity at room temperature. (a) The bar graph represents the number of motoneurons in the following experimental conditions: freshly fixed tissue (FF), sham condition, 50 μ M kainate, 0.75 μ M celastrol treated spinal cord for 6 hr or 24 hr, pretreated with 0.75 μ M celastrol followed by kainate application or 0.75 μ M celastrol applied after kainate. One-Way ANOVA followed by Holm–Sidak multiple comparisons test. $F_{6,77} = 19.24, p < 0.001^{***}$. SHAM vs KA $p < 0.001^{***}$; KA vs CE 6 hr $p < 0.001^{***}$; KA vs CE 6 hr + KA $p < 0.001^{***}$; KA vs KA + CE 24 hr $p = 0.004^{**}$. Data are mean \pm SD from four sections for each spinal cord in each experimental group comprising three spinal cords. (b) Bar graph shows the numbers of motoneurons containing nAIF in the experimental conditions described above. Following kainate, the number of motoneurons containing nAIF increased. Note the reduction in the number of motoneurons with nAIF translocation in spinal cords treated with celastrol before or after kainate. Kruskal–Wallis followed by Dunn’s multiple comparisons test. $H = 58.88, p < 0.001^{***}$. SHAM vs KA $p < 0.001^{***}$; KA vs CE 6 hr $p < 0.001^{***}$; KA vs CE 6 hr + KA $p < 0.001^{***}$; KA vs KA + CE 24 hr $p = 0.001^{**}$. Same samples as in (a). (c) Bar graph represents the average intensity of single motoneurons expressing HSP70 (HSP70 immunofluorescence signal in AU represents both constitutive and inducible form). Intensity was measured for each motoneuron in a z-stack projection with 0.5 μ m step size. One-way ANOVA followed by Holm–Sidak multiple comparisons test. $F_{6,115} = 22.73, p < 0.001^{***}$. SHAM vs CE 6 hr $p < 0.001^{***}$; SHAM vs CE 24 hr $p < 0.001^{***}$; SHAM vs CE 6 hr + KA $p < 0.001^{***}$; SHAM vs KA + CE 24 hr $p < 0.001^{***}$; KA vs CE 6 hr + KA $p < 0.001^{***}$; KA vs KA + CE 24 hr $p < 0.001^{***}$. Same samples as in (a)

marker for motoneuronal death (see also (Oh, Shin, & Kang, 2006). HSP70 is known to block cell death by binding and antagonizing AIF (Ravagnan et al., 2001). Maintenance of the spinal cord in vitro at 37°C for 6 hr (sham preparation) was associated with a small, yet significant fall (Figure 2b, approximately 20% fall) in the number of SMI32-positive (Figure 2a green, sham) motoneurons, although the average number of AIF-positive motoneurons was like control (Figure 2a red, c). The constitutive level of HSP70 was undetectable in fresh or sham tissue (Figure 2a,d). Celastrol (0.75 μ M) did not increase the number of motoneurons with nAIF, to confirm lack of toxicity (Figure 2a,b) in accordance with data in Figure 1. Figure 2d shows that after 6 hr celastrol (CE 6 hr), a detectable band of HSP70 signal was apparent (50% of the largest signal present after celastrol + kainate; CE 6 hr + KA).

Next, we investigated the effect of 0.75 μ M celastrol applied after transient kainate insult (KA + CE 6 hr). Kainate (50 μ M, 1 hr; 37°C) per se evoked a significant loss (around 22%) of SMI32-positive motoneurons (Figure 2a,b; Kuzhandaivel, Margaryan et al., 2010; Kuzhandaivel, Nistri et al., 2010) together with a large rise in the number (five-fold increase) of motoneurons with nAIF (Figure 2a,c) and undetectable HSP expression (Figure 2d) at 6 hr after injury (KA + CE 6 hr). When celastrol was applied for 6 hr

In our previous work (Bianchetti et al., 2013; Kuzhandaivel, Nistri, Mazzone, & Mladinic, 2011; Shabbir et al., 2015), we have shown that nuclear AIF (nAIF) translocation is a reliable

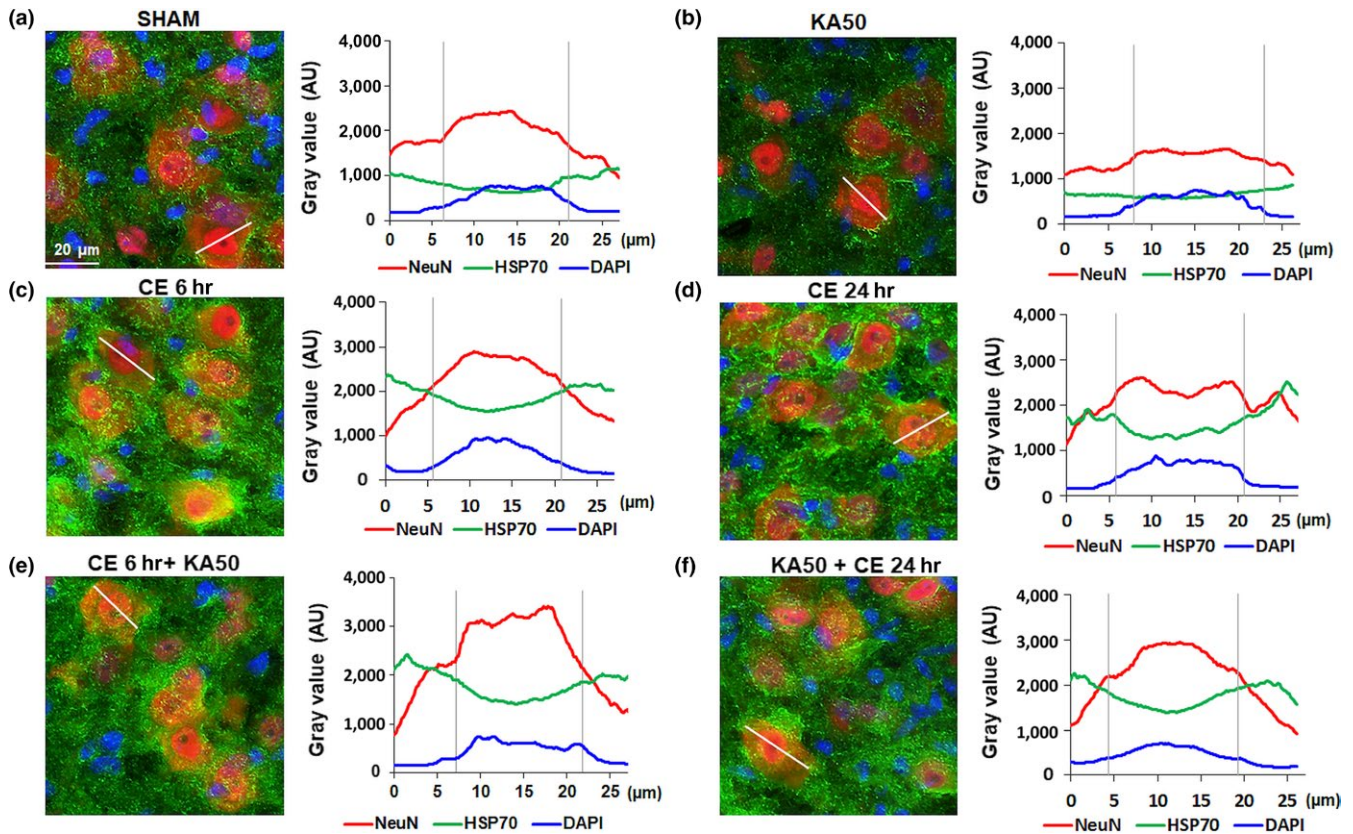


FIGURE 4 Line scan analysis of motoneurons. Spinal cord sections are immunostained for HSP70 (green) (which recognizes both constitutive and inducible form) and for neuronal nuclear marker NeuN (red) which has slight cytoplasmic distribution in the spinal cord motor neurons. Cell nuclei are stained with DAPI (blue). White lines in left panels indicate examples of line scan analysis performed on the z-stack to produce the plots depicted on the right of each panel (a–f) in which the three markers are shown in the cytoplasm and nucleus (vertical lines on the plot define nuclear expression). Line plot is average line intensity of six cells randomly taken from three spinal cords per each experimental group shown in Figure 3, using Olympus CellSens (Olympus, Tokyo, Japan). Scale bar is 20 μm . Abbreviations and protocols as in Figure 2

on washout of kainate, Figure 2a–c shows that the number of motoneurons was not significantly different from sham, although the ones expressing nAIF were more numerous (threefold increase) than in sham preparations. Furthermore, a weak HSP expression was observed corresponding to 35% of the largest signal (corresponding to preapplication of celastrol before kainate, CE 6 hr + KA; Figure 2d).

We also explored whether preapplying celastrol for 6 hr (CE 6 hr + KA) at 37°C (and, thus, enhancing HSP basal expression prior to insult; Figure 2d) could confer stronger neuroprotection against excitotoxicity. Figure 2a–c indicates that this protocol (CE 6 hr + KA) preserved the same number of motoneurons as in sham, and decreased (by over 50%) the number of those expressing nAIF and provided a robust expression of HSP.

It is a well-known fact that functional studies of *in vitro* spinal preparations are usually carried out at lower temperature. Thus, room temperature not only allows prolonged survival of the spinal cord *in vitro* (Kerkut & Bagust, 1995) but it also enables full, long-lasting operation of spinal motor networks with locomotor program output recorded

from VRs (Taccola et al., 2008). Figure S3 indicates that, unlike room temperature conditions, keeping the isolated spinal cord for 24 hr *in vitro* at 37°C (SHAM) was associated to extensive cell death, a phenomenon that could not be prevented by celastrol. We, therefore, performed further experiments for motoneuron protection at room temperature that allowed us an extended time course of observation (24 hr). Figure 3a shows that at room temperature there was no loss of motoneurons (sham) after 24 hr *in vitro*, and virtually undetectable expression of nAIF (Figure 3b) indicating effective preservation of spinal preparations under these conditions. Figure 3a,b also shows that celastrol applied for 6 or 24 hr did not induce any significant fall in motoneuron numbers or rise in AIF expression. The routinely observed loss of motoneurons (40%) or increased nAIF expression (five-fold) after 50 μM kainate application at RT to neonatal rat spinal cord *in vitro* preparation (Figure 3a,b; see also Mazzone et al., 2010) was equally contrasted (50% decrease in nAIF) by celastrol applied before (CE 6 hr + KA) or after kainate (KA + CE 24 hr). Figure 3c shows the average signal for HSP70 immunopositivity of motoneurons

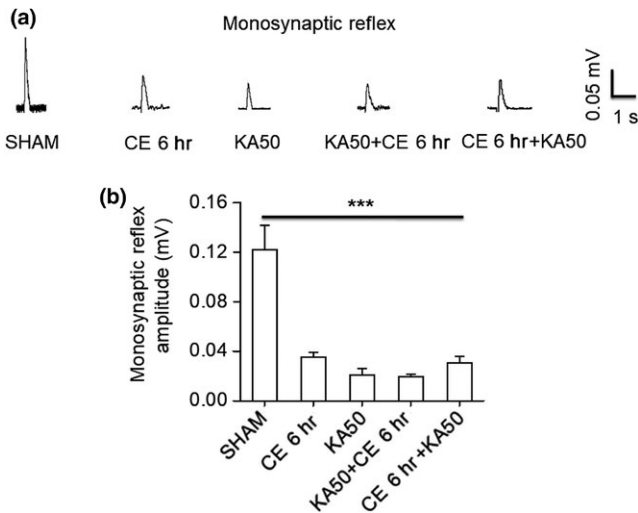


FIGURE 5 Electrophysiological effects of celastrol. (a) Effect of celastrol (6 hr treatment) and kainate (KA50) on monosynaptic reflexes recorded from L5 VR 24 hr later in SHAM (day 2 control, $n = 10$), celastrol ($0.75 \mu\text{M}$) application for 6 hr on day 1 (CE 6 hr, $n = 5$), kainate application ($50 \mu\text{M}$; KA50, $n = 8$), kainate followed by celastrol for 6 hr (KA50 + CE 6 hr, $n = 6$) and celastrol applied for 6 hr followed by kainate (CE 6 hr + KA50, $n = 6$). (b) Bar graph shows fall in monosynaptic reflex amplitude for different treatment groups in comparison to SHAM. One-Way ANOVA test followed by multiple t -test comparisons was performed ($F_{4,45} = 8.320$, $p < 0.001^{***}$). Celastrol alone application for 6 hr (CE 6 hr) strongly depressed the reflex amplitude (CE 6 hr vs SHAM $p = 0.002^{**}$, $t_{12} = 4.07$; t represents the t -test whereas the subscript value represents the degree of freedom) which is similar to the depression evoked by kainate (CE 6 hr vs KA50 $p = 0.78$, $t_{24} = -0.28$). No further significant change in reflex amplitude was observed with KA50 + CE 6 hr and CE 6 hr + KA50 in comparison to kainate alone (KA50 + CE 6 hr vs KA50 $p = 0.52$, $t_{22} = 2.15$; CE 6 hr + KA50 vs KA50 $p = 0.47$, $t_{24} = 0.73$)

following the preapplication (CE 6 hr + KA) or postapplication (KA + CE 24 hr) of celastrol. Thus, celastrol (6 or 24 hr application; CE 6 hr, CE 24 hr) significantly raised (twofold) this signal and maintained it elevated even when kainate was applied.

Figure 4 shows analysis of motoneuronal HSP70 nuclear distribution after the excitotoxic protocol with (CE 6 hr + KA; KA + CE 24 hr) or without (KA50) application of celastrol. Thus, in addition to the standard DAPI staining (blue lines in Figure 4), we also used an anti-NeuN antibody (red lines in Figure 4) that typically labels neuronal nuclei (Kim, Adelstein, & Kawamoto, 2009) and is one of the first markers altered during cell death processes (Bianchetti et al., 2013; Kuzhandaivel et al., 2011; Mazzone et al., 2010). Data were analyzed with the line scan tool of the OLYMPUS CELLSense software. Average line scans are reported in the graphs of Figure 4 alongside representative images where white lines exemplify cells used for data collection. Hence, HSP70 (green line) was located throughout the cell compartments in sham condition (Figure 4a). After celastrol

application (6 or 24 hr), there was a large rise (twofold increase) in HSP70 immunopositivity especially in the cytoplasmic compartments (Figure 4c,d). Kainate application produced a low, uniform level of HSP70 with poor NeuN signal (Figure 4b). When celastrol preceded (CE 6 hr + KA) or followed (KA + CE 24 hr) kainate application, there was a large increment (two-fold) in the HSP70 and NeuN signals (Figure 4e,f).

These data suggest that celastrol could protect motoneurons from excitotoxicity and that phenomenon was associated with a significant rise in HSP70 expression.

3.3 | Electrophysiological effects of celastrol

We next enquired the effects of celastrol on spinal networks in control conditions (SHAM) or during excitotoxicity (KA50). Celastrol ($0.75 \mu\text{M}$; 6 hr) induced a late depression of low-threshold synaptic responses (corresponding to monosynaptic reflexes; Ostroumov et al., 2007) recorded at 24 hr (Figure 5a), despite well preserved neuronal numbers (Figure 2). The amplitude depression was comparable to the one observed after 1 hr kainate. When celastrol was applied before (CE 6 hr + KA) or after (KA + CE 6 hr) kainate, there was no further change in the reflex amplitude (Figure 5a,b). Figure 6 shows that network responses evoked by stronger dorsal root pulses and comprising polysynaptic pathway activation were better preserved by application of celastrol per se in terms of peak amplitude (Figure 6a,b) although these responses became longer lasting, resulting in a large area size (Figure 6c). Neuroprotection in polysynaptic reflexes 24 hr after kainate application was modest (twofold increase), yet significant, when celastrol was administered following kainate (KA + CE 6 hr), and clearly better (fivefold increase) when this drug preceded (CE 6 hr + KA) the excitotoxic stimulus (Figure 6a–c).

To investigate the impact of celastrol on network activity, we employed two standard protocols to activate the locomotor central pattern generators and elicit alternating rhythmic discharges recorded from lumbar VRs (fictive locomotion). The first protocol consisted in applying a train of stimuli to a single dorsal root and recording the resultant cumulative depolarization of VRs with superimposed alternating rhythmic oscillations (Marchetti et al., 2001); Figure 7a). This response was also observed 24 hr after 6 hr celastrol (CE 6 hr) per se, while it was strongly decreased (almost 10 times) after kainate alone (KA50) (Figure 7a,b). Celastrol applied after kainate (KA + CE 6 hr) failed to reinstate oscillations or improve cumulative depolarization amplitude (Figure 7c) or area (Figure 7d) 24 hr later. Conversely, when celastrol preceded (CE 6 hr + KA) the excitotoxic stimulus, cumulative depolarization returned to control (sham) level (Figure 7a–c), although recovery in oscillatory activity was very small (Figure 7b).

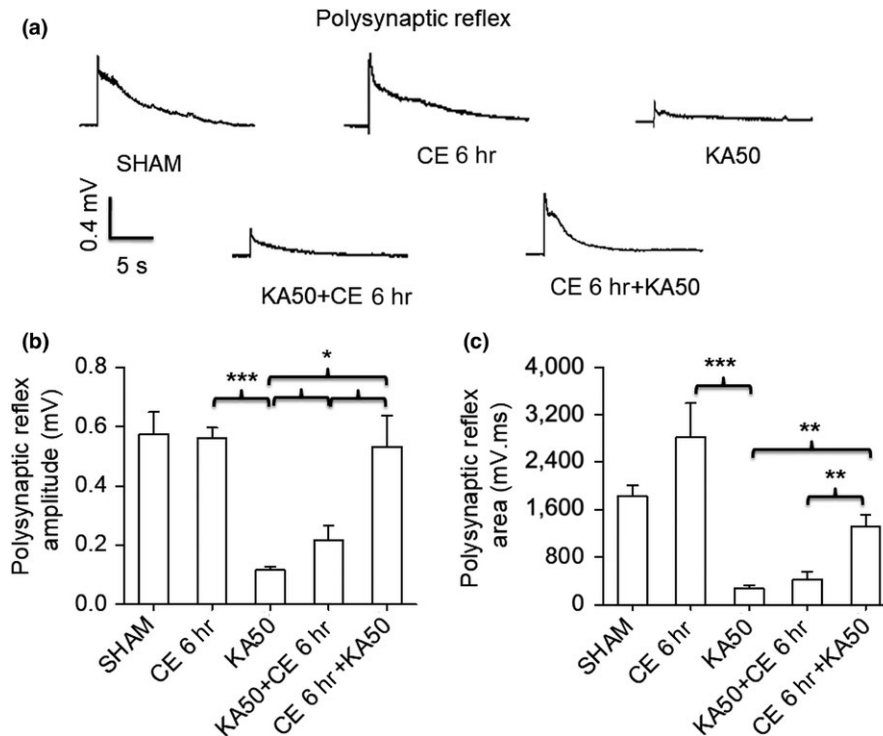


FIGURE 6 Protection by celastrol of polysynaptic reflex activity. Effect of celastrol (6 hr treatment) on polysynaptic reflex responses 24 hr after exposure to kainate induced excitotoxicity. (a) Sample records of polysynaptic reflex responses recorded from L5 VR in SHAM (day 2 control, $n = 10$), celastrol ($0.75 \mu\text{M}$) application for 6 hr on day 1 (CE 6 hr, $n = 5$), kainate application ($50 \mu\text{M}$; KA50, $n = 8$), kainate followed by celastrol for 6 hr (KA50 + CE 6 hr, $n = 6$) and celastrol applied for 6 hr followed by kainate (CE 6 hr + KA50, $n = 6$). (b, c) Bar graphs represent polysynaptic reflex amplitude (b) and area (c). One-Way ANOVA test followed by multiple t -test comparisons was performed between groups for the reflex amplitude ($F_{4,55} = 29.928$, $p < 0.001^{***}$) and area ($F_{4,60} = 13.783$, $p < 0.001^{***}$). Note a significant increase in reflex amplitude after application of kainate followed by celastrol 6 hr (KA vs KA50 + CE 6 hr $p = 0.0408^*$, $t_5 = -2.74$) with no significant change in area (KA vs KA50 + CE 6 hr $p = 0.365$, $t_6 = 1.94$) when compared with kainate alone. However, prior application of celastrol for 6 hr followed by kainate (CE 6 hr + KA50) significantly raised the amplitude (b; KA vs CE 6 hr + KA50 $p = 0.0108^*$, $t_5 = -3.95$) and area (c; KA vs CE 6 hr + KA50 $p = 0.002^{**}$, $t_6 = 1.94$) of reflex responses when compared with kainate alone (KA50)

Fictive locomotion can also be evoked by chemicals like a mixture of NMDA and 5-HT that generate sustained alternating motor patterns from VRs (Beato & Nistri, 1999; Cazalets et al., 1992; Taccola & Nistri, 2004). This rhythm was depressed 24 hr after 6 hr application of celastrol (CE 6 hr) (Figure 8a,b) as cycle amplitude fell (more than half) and periodicity increased (two-fold) while alternation among VRs was preserved (Figure 8a–c). Kainate (KA50) abolished fictive locomotion (Figure 8; see also (Mazzone et al., 2010)). Celastrol after kainate (KA + CE 6 hr) application improved (threefold increase) cycle amplitude (Figure 8b) and enabled the emergence of a rhythm that was as slow as the one detected after celastrol *per se* (CE 6 hr) (Figure 8a,c). A similar result was observed when celastrol was applied prior to kainate (CE 6 hr + KA) (Figure 8a–c). The slow rhythmicity was a stereotypic effect since changing the concentration of NMDA ($3\text{--}5 \mu\text{M}$) failed to alter the rhythm period. Hence, while celastrol could protect motoneurons from structural damage, its ability to preserve functional activity was limited to modest persistence of polysynaptic activity and slow alternating rhythmicity, though it is questionable whether it is physiologically relevant *in vivo*.

4 | DISCUSSION

The principal observation of this study is that celastrol could enhance the expression of HSP70 by motoneurons of the rat spinal cord *in vitro* and that this effect significantly contrasted the extent of excitotoxic death evoked by kainate. Nevertheless, the protection of lumbar motor networks evaluated with electrophysiological recording by celastrol was rather limited, suggesting that, despite histological preservation, a functional deficit remained, likely not only at the level of motoneurons but also pre-motoneurons.

4.1 | Selection of celastrol concentration

In this study, we tested a relatively narrow range of celastrol concentrations (0.75 , 1.5 and $3 \mu\text{M}$), which induced high expression of inducible HSP70 compared to sham preparations. These results correlate with previous studies showing that celastrol and some of its derivatives (celastrol methyl

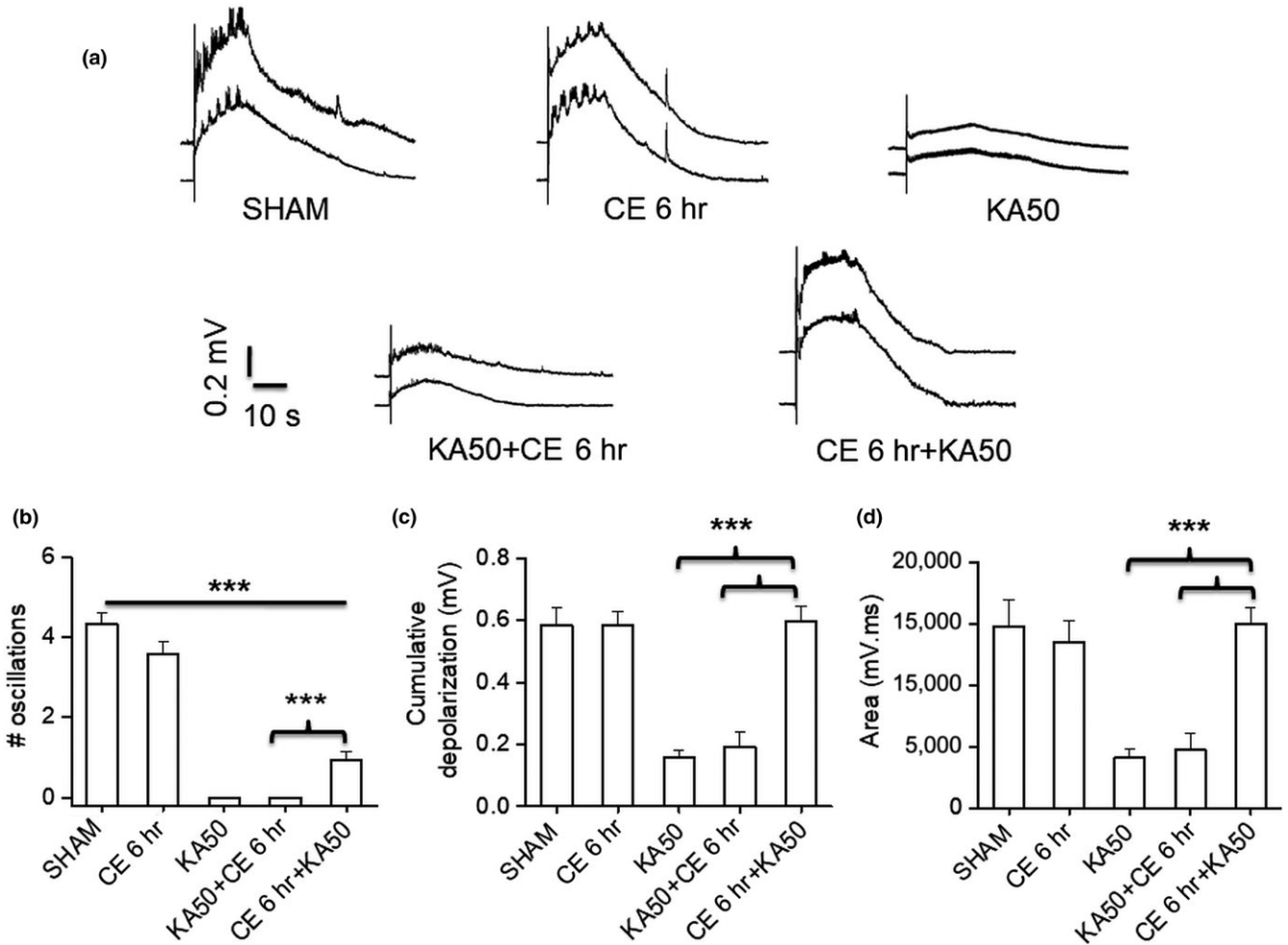


FIGURE 7 Cumulative depolarization changes induced by celastrol. Changes in cumulative depolarization and associated electrically evoked fictive locomotion (FL) after kainate-induced excitotoxicity and its treatment with celastrol (6 hr). (a) Example traces of cumulative depolarization with superimposed FL cycles for SHAM ($n = 10$), celastrol (CE 6 hr, $n = 5$), kainate (50 μ M; KA50, $n = 8$), kainate followed by celastrol for 6 hr (KA50 + CE 6 hr, $n = 6$) and celastrol applied for 6 hr followed by kainate (CE 6 hr + KA50, $n = 6$) conditions. (b–d) Bar plots illustrating the number of oscillations (b), cumulative depolarization amplitude (c), and area of cumulative depolarization (d) after application of CE 6 hr, KA 50, KA50 + CE 6 hr and CE 6 hr + KA50 in comparison to SHAM. One-Way ANOVA test followed by multiple t-test comparisons was performed between different groups for the number of oscillations ($F_{4,54} = 77.28$, $p < 0.001^{***}$), cumulative depolarization amplitude ($F_{4,61} = 24.694$, $p < 0.001^{***}$) and area of cumulative depolarization ($F_{4,60} = 12.787$, $p < 0.001^{***}$). No measurable change observed in cumulative depolarization after kainate followed by celastrol application for 6 hr (KA50 + CE 6 hr) when compared with kainate alone, whereas significant increase in the amplitude (c; $p < 0.001^{***}$, $t_{18} = -7.81$) and area (d; $p < 0.001^{***}$, $t_{19} = -7.48$) of cumulative depolarization appeared with small recovery in oscillations (b; $p < 0.001^{***}$, $t_7 = 6.78$)

ester and dihydrocelastrol diacetate) activate the heat shock response at a concentration range of 1–10 μ M (Westerheide et al., 2004).

Nevertheless, concentrations $>0.75 \mu$ M induced motoneuronal death, a toxic phenomenon apparently unrelated to HSP70 expression and whose origin remains to be studied (Chow & Brown, 2007; Kalmar & Greensmith, 2009). Likewise, it has been shown that 0.5 μ M celastrol was toxic to zebrafish embryos by inducing developmental abnormalities, while the 2 μ M concentration (24 hr) was lethal (Wang, Liu, Wang, He, & Chen, 2011). Thus, 0.75 μ M was taken as the celastrol concentration for neuroprotection analysis.

4.2 | Effect of temperature on celastrol neuroprotective action

Exploring the role of HSP in neuroprotection presents a number of challenges. First, it is necessary to find out experimental conditions that minimize tissue lesion under control conditions to avoid inadvertent induction of HSP; second, it is important to realize that HSP was discovered to be active in reaction to cell damage due to high temperature. For these reasons, we used two different temperatures (37°C and room temperature) in our experiments. It is a standard procedure to keep the isolated spinal cord preparation at room temperature to allow electrophysiological measurements (Kerkut &

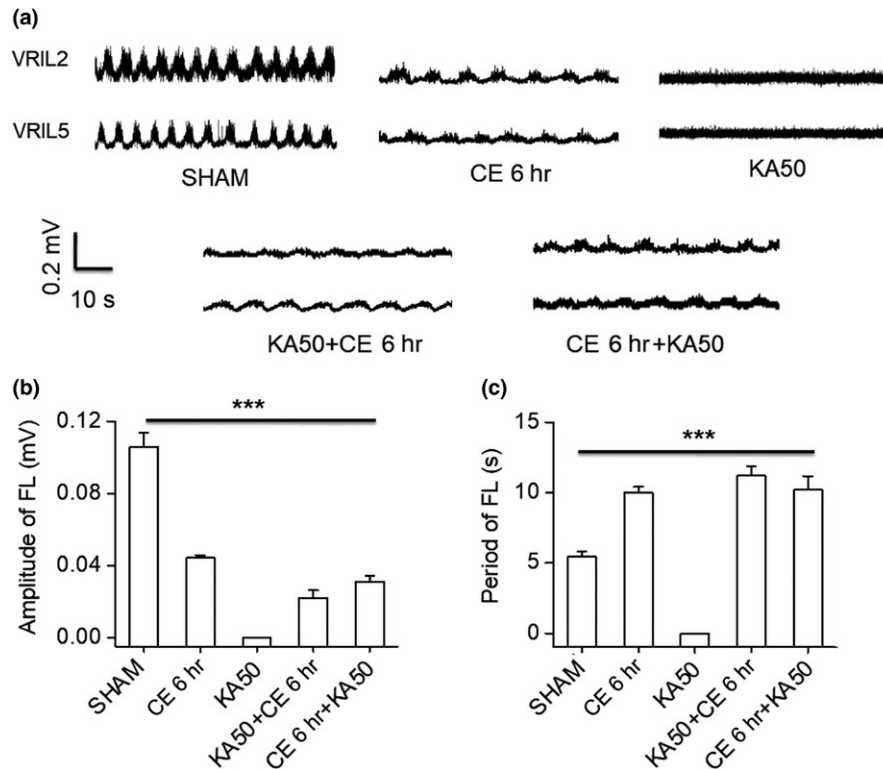


FIGURE 8 Effect of celastrol on chemically induced fictive locomotion. Recovery of chemically induced fictive locomotion (FL) either after or prior application of celastrol (CE 6 hr) and kainate (KA50). (a) Representative records of NMDA + 5HT evoked FL recorded from L2 and L5 VRs in SHAM ($n = 10$), celastrol alone applied for 6 hr (CE 6 hr, $n = 5$), kainate (50 μ M; KA50, $n = 8$), kainate followed by celastrol for 6 hr (KA50 + CE 6 hr, $n = 6$) and celastrol applied for 6 hr followed by kainate (CE 6 hr + KA50, $n = 6$). (b, c) Bar graphs show changes in cycle amplitude and periodicity of FL of all groups in comparison to SHAM. One-Way ANOVA test followed by multiple t -test comparisons was performed between all groups for the cycle amplitude ($F_{4,32} = 34.949$, $p < 0.001^{***}$) and periodicity ($F_{4,30} = 25.343$, $p < 0.001^{***}$). Celastrol per se halved the amplitude of FL (CE 6 hr vs SHAM $p < 0.001^{***}$, $t_{13} = 7.64$) with slower periodicity (CE 6 hr vs SHAM $p < 0.001^{***}$, $t_{11} = -8.53$) when compared with SHAM conditions. Kainate application completely abolished locomotor rhythmic cycles (a–c). Cycle amplitude (b) partly recovered after post- or pretreatment celastrol with kainate although with slower periodicity (c) in comparison to kainate alone (amplitude: $p < 0.001^{***}$, period: $p < 0.001^{***}$; KA50 + CE 6 hr vs KA50; CE 6 hr + KA50 vs KA50)

Bagust, 1995) so that long-lasting recording of locomotor network activity after an initial lesion is possible to explore the dynamics of motor dysfunction (Mladinic et al., 2013; Taccola et al., 2008). Indeed, even after just 6 hr at 37°C in vitro, the basal number of motoneurons had fallen, indicating nonoptimal conditions and extensive tissue degeneration was present at 24 hr. Of course, activation of HSP would be expected, in principle, to be more intense at 37°C, although in our preparation, this experimental condition severely limited the tissue viability to a few hours, a length of time too short to observe full manifestation of the secondary lesion of the spinal cord (Kuzhandaivel, Margaryan et al., 2010; Kuzhandaivel, Nistri et al., 2010). It is noteworthy that the higher temperature of 37°C did not per se stimulate HSP expression at 6 hr examined with western blotting probably because, in the whole tissue of the spinal cord, any change at the level of motoneurons and premotoneurons (which are a small minority cell population; Cifra et al., 2012) might have been diluted out.

4.3 | Celastrol application before or after kainate injury

Even though the translational impact of celastrol and related drugs should be ideally investigated when this drug is applied after the excitotoxic injury, this study also employed the preapplication of celastrol to facilitate (and confirm) its mechanism of action on HSP70 and to prevent motoneuronal death. We have shown (Kuzhandaivel, Nistri et al., 2010) that motoneuronal death starts after 4 hr from excitotoxic insult (kainate application) and to be complete at 24 hr (Mazzone, Mladinic, & Nistri, 2013). Immunohistological data indicated that celastrol was effective to neuroprotect at 6 hr (37°C) or 24 hr (room temperature) not only by maintaining a high number of motoneurons, but also by minimizing those expressing nAIF. These observations are, therefore, fully compatible with the opposite effect of the HSP inhibitor VER155008 that largely intensified the kainate damage (Shabbir et al., 2015). Hence, these results globally concur to support a neuroprotective role for HSP70.

4.4 | Mismatch between histological and functional protection

Electrophysiological recording demonstrated that significant changes in reflex activity were already seen even after applying celastrol alone as monosynaptic reflexes were depressed in amplitude while polysynaptic ones became shorter. The impairment in monosynaptic transmission remained throughout protocols of excitotoxicity and suggested that even motoneurons with apparently normal histological profile had deficient synaptic transmission. When afferent inputs were of much stronger intensity to elicit polysynaptic transmission, the depression by celastrol was less intense and it actually protected, to a degree, against kainate. This effect was similarly observed with a train of strong stimuli delivered to a single dorsal root to elicit cumulative depolarization. Future studies are necessary to investigate whether distinct subpopulations of premotoneurons were better protected by celastrol than motoneurons themselves, and, therefore, provided an improved contribution to the polysynaptic reflex pathways even though functional recovery was far from complete. Hence, we propose that, by recruiting a larger population of neurons via more intense stimulation, the depression of celastrol was partly overcome and any effect via HSP70 could be manifested. Nonetheless, cumulative depolarization was rarely accompanied by alternating oscillations typical of locomotor network activity indicating that damage to the local premotoneuron network responsible for rhythmic oscillations had occurred (Kiehn, 2006). When the stimulation of the locomotor network of the lumbar spinal cord was uniform via bath application of NMDA and 5HT, then an alternating rhythm of rather slow periodicity appeared after celastrol application before or after kainate. In this case, the extent of network activation is expected to be very large so that recruitment of additional circuitry neurons would be sufficient to reclaim rhythmicity, though unable to support effective locomotion in view of the small cycle amplitude, slow periodicity and inability to respond to varying concentrations of NMDA. It seems likely that the persisting functional deficit not only affected just motoneurons but also premotoneurons that are responsible for the rhythm generation (McCrea & Rybak, 2008). Of course, because the isolated spinal cord preparation does not allow prolonging recording after 24 hr *in vitro*, we cannot exclude that further recovery in locomotor network activity develops on a much slower time course.

4.5 | Translational implications

Clinical application of celastrol is rather limited because of its poor solubility and narrow therapeutic window (Zheng et al.,

2014). However, combined therapy of low doses of celastrol with other agents could represent a novel, efficient strategy with acceptable toxicity to treat cancer (Chen et al., 2018; Zheng et al., 2014). These data suggest potential avenues to be explored in future also for neuroprotection. In particular, arimocloamol (commercially unavailable at the time of the present experiments) is also reported to enhance HSP70 expression (Kalmar & Greensmith, 2009; Keppel Hesselink, 2016) with lower toxicity (Kalmar & Greensmith, 2009) and its effect on spinal injury deserves to be studied.

5 | CONCLUSIONS

The present results show that, while HSP70 may be neuroprotective for motoneurons, the role of this mechanism is likely to be constrained by a temporal mismatch between lesion progression and HSP upregulation. Nevertheless, our study has considered only one of the celastrol mechanisms of action (HSP upregulation), whereas other actions could also be relevant such as, for example, its anti-inflammatory role (Jiang et al., 2018), since neuroinflammation is a major contributor to chronic spinal cord injury (Alexander & Popovich, 2009; Hausmann, 2003; Okada, 2016; Schwab et al., 2006).

ACKNOWLEDGEMENTS

This work was supported by an SISSA intramural grant to AN, the ICGEB Research Grant CRP/CRO14-03 to MM and Croatian Science Foundation Research Grant IP-2016-06-7060 to MM. Microscopy infrastructure was provided by the project RISK “Development of University of Rijeka campus laboratory research infrastructure” financed by the European Regional Development Fund.

CONFLICT OF INTEREST

All authors declare no conflicts of interests.

DATA ACCESSIBILITY

Manuscript's supporting data can be accessed in the online submission system of European Journal of Neuroscience in the form of Data Files and Supporting Information.

AUTHORS' CONTRIBUTIONS

All authors approved the final manuscript. Conception and design of the work AP, JK, AN, MM; acquisition and analysis of data, AP, JK, IT; interpretation of data, AP, JK, AN, MM; wrote/revised the manuscript, AP, AN, MM. The authors declare no competing interests.

ORCID

Andrea Nistri  <https://orcid.org/0000-0002-0638-0900>

Miranda Mladinic  <https://orcid.org/0000-0002-3985-6629>

REFERENCES

- Ahuja, C. S., Nori, S., Tetreault, L., Wilson, J., Kwon, B., Harrop, J., ... Fehlings, M. G. (2017). Traumatic spinal cord injury-repair and regeneration. *Neurosurgery*, *80*, S9–S22. <https://doi.org/10.1093/neuros/nyw080>
- Alexander, J. K., & Popovich, P. G. (2009). Neuroinflammation in spinal cord injury: Therapeutic targets for neuroprotection and regeneration. *Progress in Brain Research*, *175*, 125–137. [https://doi.org/10.1016/S0079-6123\(09\)17508-8](https://doi.org/10.1016/S0079-6123(09)17508-8)
- Allison, A. C., Cacabelos, R., Lombardi, V. R., Alvarez, X. A., & Vigo, C. (2001). Celastrol, a potent antioxidant and anti-inflammatory drug, as a possible treatment for Alzheimer's disease. *Progress in Neuro-Psychopharmacology and Biological Psychiatry*, *25*, 1341–1357. [https://doi.org/10.1016/S0278-5846\(01\)00192-0](https://doi.org/10.1016/S0278-5846(01)00192-0)
- Awad, H., Suntres, Z., Heijmans, J., Smeak, D., Bergdall-Costell, V., Christofi, F. L., ... Oglesbee, M. (2008). Intracellular and extracellular expression of the major inducible 70 kDa heat shock protein in experimental ischemia-reperfusion injury of the spinal cord. *Experimental Neurology*, *212*, 275–284. <https://doi.org/10.1016/j.expneurol.2008.03.024>
- Batulan, Z., Shinder, G. A., Minotti, S., He, B. P., Doroudchi, M. M., Nalbantoglu, J., ... Durham, H. D. (2003). High threshold for induction of the stress response in motor neurons is associated with failure to activate HSF1. *Journal of Neuroscience*, *23*, 5789–5798. <https://doi.org/10.1523/JNEUROSCI.23-13-05789.2003>
- Beato, M., & Nistri, A. (1999). Interaction between disinhibited bursting and fictive locomotor patterns in the rat isolated spinal cord. *Journal of Neurophysiology*, *82*, 2029–2038. <https://doi.org/10.1152/jn.1999.82.5.2029>
- Bianchetti, E., Mladinic, M., & Nistri, A. (2013). Mechanisms underlying cell death in ischemia-like damage to the rat spinal cord in vitro. *Cell Death & Disease*, *4*, e707. <https://doi.org/10.1038/cddis.2013.237>
- Boridy, S., Le, P. U., Petrecca, K., & Maysinger, D. (2014). Celastrol targets proteostasis and acts synergistically with a heat-shock protein 90 inhibitor to kill human glioblastoma cells. *Cell Death & Disease*, *5*, e1216. <https://doi.org/10.1038/cddis.2014.182>
- Cascão, R., Fonseca, J. E., & Moita, L. F. (2017). Celastrol: A spectrum of treatment opportunities in chronic diseases. *Frontiers in Medicine*, *4*, 69. <https://doi.org/10.3389/fmed.2017.00069>
- Cazalets, J. R., Sqalli-Houssaini, Y., & Clarac, F. (1992). Activation of the central pattern generators for locomotion by serotonin and excitatory amino acids in neonatal rat. *Journal of Physiology*, *455*, 187–204. <https://doi.org/10.1113/jphysiol.1992.sp019296>
- Chen, S.-R., Dai, Y., Zhao, J., Lin, L., Wang, Y., & Wang, Y. (2018). Mechanistic overview of triptolide and celastrol, natural products from *Tripterygium wilfordii* Hook F. *Frontiers in Pharmacology*, *9*, 104. <https://doi.org/10.3389/fphar.2018.00104>
- Chow, A. M., & Brown, I. R. (2007). Induction of heat shock proteins in differentiated human and rodent neurons by celastrol. *Cell Stress and Chaperones*, *12*, 237–244. <https://doi.org/10.1379/CSC-269.1>
- Cifra, A., Mazzone, G. L., Nani, F., Nistri, A., & Mladinic, M. (2012). Postnatal developmental profile of neurons and glia in motor nuclei of the brainstem and spinal cord, and its comparison with organotypic slice cultures. *Developmental Neurobiology*, *72*, 1140–1160. <https://doi.org/10.1002/dneu.20991>
- Deane, C. A. S., & Brown, I. R. (2018). Knockdown of heat shock proteins HSPA6 (Hsp70B') and HSPA1A (Hsp70-1) sensitizes differentiated human neuronal cells to cellular stress. *Neurochemical Research*, *43*, 340–350. <https://doi.org/10.1007/s11064-017-2429-z>
- Dell'Anno, M. T., & Strittmatter, S. M. (2017). Rewiring the spinal cord: Direct and indirect strategies. *Neuroscience Letters*, *652*, 25–34. <https://doi.org/10.1016/j.neulet.2016.12.002>
- DeMeester, S. L., Buchman, T. G., & Cobb, J. P. (2001). The heat shock paradox: Does NF-kappaB determine cell fate?. *The FASEB Journal*, *15*, 270–274. <https://doi.org/10.1096/fj.00-0170hyp>
- Deng, Y.-N., Shi, J., Liu, J., & Qu, Q.-M. (2013). Celastrol protects human neuroblastoma SH-SY5Y cells from rotenone-induced injury through induction of autophagy. *Neurochemistry International*, *63*, 1–9. <https://doi.org/10.1016/j.neuint.2013.04.005>
- Deumens, R., Mazzone, G. L., & Taccola, G. (2013). Early spread of hyperexcitability to caudal dorsal horn networks after a chemically-induced lesion of the rat spinal cord in vitro. *Neuroscience*, *229*, 155–163. <https://doi.org/10.1016/j.neuroscience.2012.10.036>
- Faust, K., Gehrke, S., Yang, Y., Yang, L., Beal, M. F., & Lu, B. (2009). Neuroprotective effects of compounds with antioxidant and anti-inflammatory properties in a Drosophila model of Parkinson's disease. *BMC Neuroscience*, *10*, 109. <https://doi.org/10.1186/1471-2202-10-109>
- Filous, A. R., & Schwab, J. M. (2018). Determinants of axon growth, plasticity, and regeneration in the context of spinal cord injury. *American Journal of Pathology*, *188*, 53–62. <https://doi.org/10.1016/j.ajpath.2017.09.005>
- Fleshner, M., & Johnson, J. D. (2005). Endogenous extra-cellular heat shock protein 72: Releasing signal(s) and function. *International Journal of Hyperthermia*, *21*, 457–471. <https://doi.org/10.1080/02656730500088211>
- Fulton, B. P., & Walton, K. (1986). Electrophysiological properties of neonatal rat motoneurons studied in vitro. *Journal of Physiology*, *370*, 651–678. <https://doi.org/10.1113/jphysiol.1986.sp015956>
- Gu, L., Kwong, J. M. K., Yadegari, D., Yu, F., Caprioli, J., & Piri, N. (2018). The effect of celastrol on the ocular hypertension-induced degeneration of retinal ganglion cells. *Neuroscience Letters*, *670*, 89–93. <https://doi.org/10.1016/j.neulet.2018.01.043>
- Hausmann, O. N. (2003). Post-traumatic inflammation following spinal cord injury. *Spinal Cord*, *41*, 369–378. <https://doi.org/10.1038/sj.sc.3101483>
- Hoh, D. J., Mercier, L. M., Hussey, S. P., & Lane, M. A. (2013). Respiration following spinal cord injury: Evidence for human neuroplasticity. *Respiratory Physiology & Neurobiology*, *189*, 450–464. <https://doi.org/10.1016/j.resp.2013.07.002>
- Jantas, D., Roman, A., Kuśmierczyk, J., Lorenc-Koci, E., Konieczny, J., Lenda, T., & Lasoń, W. (2013). The extent of neurodegeneration and neuroprotection in two chemical in vitro models related to Parkinson's disease is critically dependent on cell culture conditions. *Neurotoxicity Research*, *24*, 41–54. <https://doi.org/10.1007/s12640-012-9374-z>
- Jiang, M., Liu, X., Zhang, D., Wang, Y., Hu, X., Xu, F., ... Xu, L. (2018). Celastrol treatment protects against acute ischemic stroke-induced brain injury by promoting an IL-33/ST2 axis-mediated microglia/

- macrophage M2 polarization. *Journal of Neuroinflammation*, *15*, 78. <https://doi.org/10.1186/s12974-018-1124-6>
- Kaelan, C., Jacobsen, P. F., & Kakulas, B. A. (1988). An investigation of possible transynaptic neuronal degeneration in human spinal cord injury. *Journal of the Neurological Sciences*, *86*, 231–237. [https://doi.org/10.1016/0022-510X\(88\)90101-3](https://doi.org/10.1016/0022-510X(88)90101-3)
- Kalmar, B., & Greensmith, L. (2009). Activation of the heat shock response in a primary cellular model of motoneuron neurodegeneration—evidence for neuroprotective and neurotoxic effects. *Cellular & Molecular Biology Letters*, *14*, 319–335.
- Kannaiyan, R., Shanmugam, M. K., & Sethi, G. (2011). Molecular targets of celastrol derived from Thunder of God Vine: Potential role in the treatment of inflammatory disorders and cancer. *Cancer Letters*, *303*, 9–20. <https://doi.org/10.1016/j.canlet.2010.10.025>
- Kaur, J., Rauti, R., & Nistri, A. (2018). Nicotine-mediated neuroprotection of rat spinal networks against excitotoxicity. *European Journal of Neuroscience*, *47*, 1353–1374. <https://doi.org/10.1111/ejn.13950>
- Keppel Hesselink, J. M. (2016). Bimoclochol and arimoclochol: HSP-co-inducers for the treatment of protein misfolding disorders, neuropathy and neuropathic pain. *Journal of Pain & Relief*, *6*, 1–5.
- Kerkut, G. A., & Bagust, J. (1995). The isolated mammalian spinal cord. *Progress in Neurobiology*, *46*, 1–48. [https://doi.org/10.1016/0301-0082\(94\)00055-M](https://doi.org/10.1016/0301-0082(94)00055-M)
- Kiehn, O. (2006). Locomotor circuits in the mammalian spinal cord. *Annual Review of Neuroscience*, *29*, 279–306. <https://doi.org/10.1146/annurev.neuro.29.051605.112910>
- Kim, K. K., Adelstein, R. S., & Kawamoto, S. (2009). Identification of Neuronal Nuclei (NeuN) as Fox-3, a new member of the Fox-1 gene family of splicing factors. *Journal of Biological Chemistry*, *284*, 31052–31061. <https://doi.org/10.1074/jbc.M109.052969>
- Krnjević, K., Lamour, Y., MacDonald, J. F., & Nistri, A. (1979). Depression of monosynaptic excitatory postsynaptic potentials by Mn^{2+} and Co^{2+} in cat spinal cord. *Neuroscience*, *4*, 1331–1339. [https://doi.org/10.1016/0306-4522\(79\)90160-X](https://doi.org/10.1016/0306-4522(79)90160-X)
- Kuzhandaivel, A., Margaryan, G., Nistri, A., & Mladinic, M. (2010). Extensive glial apoptosis develops early after hypoxic-dysmetabolic insult to the neonatal rat spinal cord in vitro. *Neuroscience*, *169*, 325–338. <https://doi.org/10.1016/j.neuroscience.2010.05.011>
- Kuzhandaivel, A., Nistri, A., Mazzone, G. L., & Mladinic, M. (2011). Molecular mechanisms underlying cell death in spinal networks in relation to locomotor activity after acute injury in vitro. *Frontiers in Cellular Neuroscience*, *5*, 9.
- Kuzhandaivel, A., Nistri, A., & Mladinic, M. (2010). Kainate-mediated excitotoxicity induces neuronal death in the rat spinal cord in vitro via a PARP-1 dependent cell death pathway (Parthanatos). *Cellular and Molecular Neurobiology*, *30*, 1001–1012. <https://doi.org/10.1007/s10571-010-9531-y>
- Kyung, H., Kwong, J. M. K., Bekerman, V., Gu, L., Yadegari, D., Caprioli, J., & Piri, N. (2015). Celastrol supports survival of retinal ganglion cells injured by optic nerve crush. *Brain Research*, *1609*, 21–30. <https://doi.org/10.1016/j.brainres.2015.03.032>
- Marchetti, C., Beato, M., & Nistri, A. (2001). Alternating rhythmic activity induced by dorsal root stimulation in the neonatal rat spinal cord in vitro. *Journal of Physiology*, *530*, 105–112. <https://doi.org/10.1111/j.1469-7793.2001.0105m.x>
- Margaryan, G., Mattioli, C., Mladinic, M., & Nistri, A. (2010). Neuroprotection of locomotor networks after experimental injury to the neonatal rat spinal cord in vitro. *Neuroscience*, *165*, 996–1010. <https://doi.org/10.1016/j.neuroscience.2009.10.066>
- Margaryan, G., Mladinic, M., Mattioli, C., & Nistri, A. (2009). Extracellular magnesium enhances the damage to locomotor networks produced by metabolic perturbation mimicking spinal injury in the neonatal rat spinal cord in vitro. *Neuroscience*, *163*, 669–682. <https://doi.org/10.1016/j.neuroscience.2009.07.005>
- Mazzone, G. L., Margaryan, G., Kuzhandaivel, A., Nasrabad, S. E., Mladinic, M., & Nistri, A. (2010). Kainate-induced delayed onset of excitotoxicity with functional loss unrelated to the extent of neuronal damage in the in vitro spinal cord. *Neuroscience*, *168*, 451–462. <https://doi.org/10.1016/j.neuroscience.2010.03.055>
- Mazzone, G. L., Mladinic, M., & Nistri, A. (2013). Excitotoxic cell death induces delayed proliferation of endogenous neuroprogenitor cells in organotypic slice cultures of the rat spinal cord. *Cell Death & Disease*, *4*, e902. <https://doi.org/10.1038/cddis.2013.431>
- McCrea, D. A., & Rybak, I. A. (2008). Organization of mammalian locomotor rhythm and pattern generation. *Brain Research Reviews*, *57*, 134–146. <https://doi.org/10.1016/j.brainresrev.2007.08.006>
- Mehta, A., Prabhakar, M., Kumar, P., Deshmukh, R., & Sharma, P. L. (2013). Excitotoxicity: Bridge to various triggers in neurodegenerative disorders. *European Journal of Pharmacology*, *698*, 6–18. <https://doi.org/10.1016/j.ejphar.2012.10.032>
- Mladinic, M., Bianchetti, E., Dekanic, A., Mazzone, G. L., & Nistri, A. (2014). ATF3 is a novel nuclear marker for migrating ependymal stem cells in the rat spinal cord. *Stem Cell Research*, *12*, 815–827. <https://doi.org/10.1016/j.scr.2014.03.006>
- Mladinic, M., Nistri, A., & Taccola, G. (2013). Acute spinal cord injury in vitro: insight into basic mechanisms. In H. Aldskogius (Ed.), *Animal models of spinal cord repair* (pp. 39–62). Totowa, NJ: Humana Press. <https://doi.org/10.1007/978-1-62703-197-4>
- Muchowski, P. J. (2002). Protein misfolding, amyloid formation, and neurodegeneration: A critical role for molecular chaperones? *Neuron*, *35*, 9–12. [https://doi.org/10.1016/S0896-6273\(02\)00761-4](https://doi.org/10.1016/S0896-6273(02)00761-4)
- Muchowski, P. J., & Wacker, J. L. (2005). Modulation of neurodegeneration by molecular chaperones. *Nature Reviews Neuroscience*, *6*, 11–22. <https://doi.org/10.1038/nrn1587>
- Nasrabad, S. E., Kuzhandaivel, A., Mladinic, M., & Nistri, A. (2011). Effects of 6(5H)-phenanthridinone, an inhibitor of poly(ADP-ribose)polymerase-1 activity (PARP-1), on locomotor networks of the rat isolated spinal cord. *Cellular and Molecular Neurobiology*, *31*, 503–508. <https://doi.org/10.1007/s10571-011-9661-x>
- Oh, Y. K., Shin, K. S., & Kang, S. J. (2006). AIF translocates to the nucleus in the spinal motor neurons in a mouse model of ALS. *Neuroscience Letters*, *406*, 205–210. <https://doi.org/10.1016/j.neulet.2006.07.044>
- Okada, S. (2016). The pathophysiological role of acute inflammation after spinal cord injury. *Inflammation and Regeneration*, *36*, 20. <https://doi.org/10.1186/s41232-016-0026-1>
- Ostroumov, K., Grandolfo, M., & Nistri, A. (2007). The effects induced by the sulphonylurea glibenclamide on the neonatal rat spinal cord indicate a novel mechanism to control neuronal excitability and inhibitory neurotransmission. *British Journal of Pharmacology*, *150*, 47–57.
- Park, E., Velumian, A. A., & Fehlings, M. G. (2004). The role of excitotoxicity in secondary mechanisms of spinal cord injury: A review with an emphasis on the implications for white matter degeneration. *Journal of Neurotrauma*, *21*, 754–774. <https://doi.org/10.1089/0897715041269641>
- Quraishie, S., Forbes, L. H., & Andrews, M. R. (2018). The extracellular environment of the CNS: Influence on plasticity, sprouting, and axonal regeneration after spinal cord injury. *Neural Plasticity*, *2018*, 2952386.

- Ran, R., Lu, A., Zhang, L., Tang, Y., Zhu, H., Xu, H., ... Sharp, F. R. (2004). Hsp70 promotes TNF-mediated apoptosis by binding IKK gamma and impairing NF-kappa B survival signaling. *Genes & Development, 18*, 1466–1481. <https://doi.org/10.1101/gad.1188204>
- Ravagnan, L., Gurbuxani, S., Susin, S. A., Maise, C., Daugas, E., Zamzami, N., ... Kroemer, G. (2001). Heat-shock protein 70 antagonizes apoptosis-inducing factor. *Nature Cell Biology, 3*, 839–843. <https://doi.org/10.1038/ncb0901-839>
- Reddy, S. J., La Marca, F., & Park, P. (2008). The role of heat shock proteins in spinal cord injury: Review article. *Neurosurgical Focus, 25*, E4. <https://doi.org/10.3171/FOC.2008.25.11.E4>
- Robinson, M. B. (2005). Extracellular heat shock protein 70: A critical component for motoneuron survival. *Journal of Neuroscience, 25*, 9735–9745. <https://doi.org/10.1523/JNEUROSCI.1912-05.2005>
- Salminen, A., Lehtonen, M., Paimela, T., & Kaarniranta, K. (2010). Celastrol: Molecular targets of Thunder God Vine. *Biochemical and Biophysical Research Communications, 394*, 439–442. <https://doi.org/10.1016/j.bbrc.2010.03.050>
- Schwab, J. M., Brechtel, K., Mueller, C.-A., Failli, V., Kaps, H.-P., Tuli, S. K., & Schluesener, H. J. (2006). Experimental strategies to promote spinal cord regeneration—an integrative perspective. *Progress in Neurobiology, 78*, 91–116. <https://doi.org/10.1016/j.pneurobio.2005.12.004>
- Shabbir, A., Bianchetti, E., Cargonja, R., Petrovic, A., Mladinic, M., Pilipović, K., & Nistri, A. (2015). Role of HSP70 in motoneuron survival after excitotoxic stress in a rat spinal cord injury model in vitro. *European Journal of Neuroscience, 42*, 3054–3065. <https://doi.org/10.1111/ejn.13108>
- Squair, J. W., West, C. R., & Krassioukov, A. V. (2015). Neuroprotection, plasticity manipulation, and regenerative strategies to improve cardiovascular function following spinal cord injury. *Journal of Neurotrauma, 32*, 609–621. <https://doi.org/10.1089/neu.2014.3743>
- Sun, H., Xu, L., Yu, P., Jiang, J., Zhang, G., & Wang, Y. (2010). Synthesis and preliminary evaluation of neuroprotection of celastrol analogues in PC12 cells. *Bioorganic & Medicinal Chemistry Letters, 20*, 3844–3847. <https://doi.org/10.1016/j.bmcl.2010.05.066>
- Taccola, G., Margaryan, G., Mladinic, M., & Nistri, A. (2008). Kainate and metabolic perturbation mimicking spinal injury differentially contribute to early damage of locomotor networks in the in vitro neonatal rat spinal cord. *Neuroscience, 155*, 538–555. <https://doi.org/10.1016/j.neuroscience.2008.06.008>
- Taccola, G., Mladinic, M., & Nistri, A. (2010). Dynamics of early locomotor network dysfunction following a focal lesion in an in vitro model of spinal injury. *European Journal of Neuroscience, 31*, 60–78. <https://doi.org/10.1111/j.1460-9568.2009.07040.x>
- Taccola, G., & Nistri, A. (2004). Low micromolar concentrations of 4-aminopyridine facilitate fictive locomotion expressed by the rat spinal cord in vitro. *Neuroscience, 126*, 511–520. <https://doi.org/10.1016/j.neuroscience.2004.03.045>
- Taccola, G., & Nistri, A. (2005). Characteristics of the electrical oscillations evoked by 4-aminopyridine on dorsal root fibers and their relation to fictive locomotor patterns in the rat spinal cord in vitro. *Neuroscience, 132*, 1187–1197. <https://doi.org/10.1016/j.neuroscience.2005.02.012>
- Taccola, G., & Nistri, A. (2006). Fictive locomotor patterns generated by tetraethylammonium application to the neonatal rat spinal cord in vitro. *Neuroscience, 137*, 659–670. <https://doi.org/10.1016/j.neuroscience.2005.09.025>
- Traynor, B. J., Bruijn, L., Conwit, R., Beal, F., O'Neill, G., Fagan, S. C., & Cudkovicz, M. E. (2006). Neuroprotective agents for clinical trials in ALS: A systematic assessment. *Neurology, 67*, 20–27. <https://doi.org/10.1212/01.wnl.0000223353.34006.54>
- Trott, A., West, J. D., Klaić, L., Westerheide, S. D., Silverman, R. B., Morimoto, R. I., & Morano, K. A. (2008). Activation of heat shock and antioxidant responses by the natural product celastrol: Transcriptional signatures of a thiol-targeted molecule. *Molecular Biology of the Cell, 19*, 1104–1112. <https://doi.org/10.1091/mbc.e07-10-1004>
- Turturici, G., Sconzo, G., & Geraci, F. (2011). Hsp70 and its molecular role in nervous system diseases. *Biochemistry Research International, 2011*, 618127.
- Tytell, M. (2005). Release of heat shock proteins (Hsps) and the effects of extracellular Hsps on neural cells and tissues. *International Journal of Hyperthermia, 21*, 445–455. <https://doi.org/10.1080/02656730500041921>
- Wang, S., Liu, K., Wang, X., He, Q., & Chen, X. (2011). Toxic effects of celastrol on embryonic development of zebrafish (*Danio rerio*). *Drug and Chemical Toxicology, 34*, 61–65. <https://doi.org/10.3109/01480545.2010.494664>
- Welsh, F. A., Moyer, D. J., & Harris, V. A. (1992). Regional expression of heat shock protein-70 mRNA and c-fos mRNA following focal ischemia in rat brain. *Journal of Cerebral Blood Flow & Metabolism, 12*, 204–212. <https://doi.org/10.1038/jcbfm.1992.30>
- Westerheide, S. D., Bosman, J. D., Mbadugha, B. N. A., Kawahara, T. L. A., Matsumoto, G., Kim, S., ... Morimoto, R. I. (2004). Celastrols as inducers of the heat shock response and cytoprotection. *Journal of Biological Chemistry, 279*, 56053–56060. <https://doi.org/10.1074/jbc.M409267200>
- Xu, C., Wang, X., Gu, C., Zhang, H., Zhang, R., Dong, X., ... Chen, L. (2017). Celastrol ameliorates Cd-induced neuronal apoptosis by targeting NOX2-derived ROS-dependent PP5-JNK signaling pathway. *Journal of Neurochemistry, 141*, 48–62. <https://doi.org/10.1111/jnc.13966>
- Zhang, T., Hamza, A., Cao, X., Wang, B., Yu, S., Zhan, C.-G., & Sun, D. (2008). A novel Hsp90 inhibitor to disrupt Hsp90/Cdc37 complex against pancreatic cancer cells. *Molecular Cancer Therapeutics, 7*, 162–170. <https://doi.org/10.1158/1535-7163.MCT-07-0484>
- Zhang, R., Zhang, N., Zhang, H., Liu, C., Dong, X., Wang, X., ... Chen, L. (2017). Celastrol prevents cadmium-induced neuronal cell death by blocking reactive oxygen species-mediated mammalian target of rapamycin pathway. *British Journal of Pharmacology, 174*, 82–100. <https://doi.org/10.1111/bph.13655>
- Zheng, L., Fu, Y., Zhuang, L., Gai, R., Ma, J., Lou, J., ... Yang, B. (2014). Simultaneous NF-κB inhibition and E-cadherin upregulation mediate mutually synergistic anticancer activity of celastrol and SAHA in vitro and in vivo. *International Journal of Cancer, 135*, 1721–1732. <https://doi.org/10.1002/ijc.28810>

How to cite this article: Petrović A, Kaur J, Tomljanović I, Nistri A, Mladinic M. Pharmacological induction of Heat Shock Protein 70 by celastrol protects motoneurons from excitotoxicity in rat spinal cord in vitro. *Eur J Neurosci.* 2018;00:1–17. <https://doi.org/10.1111/ejn.14218>